

Comparison of satellite ozone observations in coincident air masses in early November 1994

G. L. Manney,^{1,2} H. A. Michelsen,³ R. M. Bevilacqua,⁴ M. R. Gunson,¹ F. W. Irion,¹ N. J. Livesey,¹ J. Oberheide,⁵ M. Riese,⁵ J. M. Russell III,⁶ G. C. Toon,¹ and J. M. Zawodny⁷

Abstract. Ozone observed by seven satellite instruments, the Atmospheric Trace Molecule Spectroscopy instrument (ATMOS), Stratospheric Aerosol and Gas Experiment (SAGE) II, Polar Ozone and Aerosol Measurement (POAM) II instrument, Halogen Occultation Experiment (HALOE), Microwave Limb Sounder (MLS), Cryogenic Infrared Spectrometers and Telescopes for the Atmosphere (CRISTA), and Millimeter-wave Atmospheric Sounder (MAS), during early November 1994 is mapped in equivalent latitude/potential temperature (EqL/θ) space to facilitate nearly global comparisons of measurements taken in similar air masses. Ozone from all instruments usually agrees to within 0.5 ppmv ($\sim 5\%$) in the upper stratosphere and ~ 0.25 ppmv in the lower stratosphere; larger differences in the midstratosphere are primarily due to sampling differences. Individual profile comparisons, selected to match meteorological conditions, show remarkably good agreement between all instruments that sample similar latitudes, although some small differences do not appear to be related to sampling differences. In the Southern Hemisphere (SH) midstratosphere, the instruments (ATMOS, SAGE II, and POAM II) with observations confined to high latitudes measured low EqLs in air drawn up from low latitudes that had formed a “low-ozone pocket”; they measured much lower ozone at low EqL than those that sampled low latitudes. A low-ozone pocket had also formed in the Northern Hemisphere (NH) midstratosphere (a month earlier than this phenomenon has previously been reported), also resulting in differences between instruments based on their sampling patterns. POAM II sampled only high latitudes in the NH, where extravortex sampling did not include tropical, high-ozone air, and thus measured lower ozone at a given EqL than other instruments. Ozone laminae appear in coincident profiles from multiple instruments, confirming atmospheric origins for these features and agreement in some detail between ozone observed by several instruments; reverse trajectory calculations indicate such laminae arise from filamentation in and around the polar vortices. Both EqL/θ and profile comparisons indicate overall excellent agreement in ozone observed by all seven instruments in early November 1994. When care is taken to compare similar air masses and to understand sampling effects, much useful information can be obtained from comparisons between instruments with very different observing patterns.

1. Introduction

Understanding the consistency and reliability of stratospheric ozone profile data is of key importance to studies of ozone chemistry, stratospheric ozone trends, and assessment of effects of climate change on the stratosphere [World Meteorological Organization (WMO), 1999; *Stratospheric Processes and Their Role in Climate* (SPARC), 1998]. In recent years, there have typically been several satellite instruments operating simultaneously, albeit with differing sampling patterns, measurement techniques, and vertical resolutions. Data from some of these instruments have already been used in ozone trend studies [e.g., SPARC, 1998, and references therein] or for constructing ozone climatologies [e.g., Wang *et al.*, 1999].

The Atmospheric Laboratory for Applications and Science (ATLAS)-3 space-shuttle mission, November 3–12, 1994, provided a unique opportunity for intercomparison of satellite ozone observations. The Atmospheric Trace Molecule Spectroscopy (ATMOS) instrument, Cryogenic Infrared Spectrometers and Telescopes for the Atmosphere (CRISTA), and Millimeter-wave Atmospheric Sounder (MAS) flew on the space shuttle as part of this mission. The Upper Atmosphere Research Satellite (UARS) Microwave Limb Sounder (MLS) and Halogen Occultation Experiment (HALOE) instruments measured ozone during this time. The Stratospheric Aerosol and Gas Experiment (SAGE) II and Polar Ozone and Aerosol Measurement (POAM) II instruments were also operating. These seven limb-viewing instruments comprise visible and/or infrared (ATMOS, CRISTA, SAGE II, HALOE, POAM II) and microwave (MLS, MAS) observations, and both limb-emission (CRISTA, MLS, MAS) and solar occultation (ATMOS, SAGE II, POAM II, HALOE) observational modes, and flew on several platforms with different orbits. Most of these instruments' data have recently been reprocessed with new versions of the retrieval software. Although ozone from several of these instruments has previously been compared with one or a few of the others [e.g., Cunnold *et al.*, 1996; Froidevaux *et al.*, 1996; Rusch *et al.*, 1997; Daehler *et al.*, 1998; Riese *et al.*, 1999, and references therein], these com-

parisons used earlier data versions, and consisted primarily of comparisons of zonal means and/or limited sets of spatially and temporally coincident profiles.

Because of the different sampling patterns, spatial resolution, and coverage, it is often difficult to compare observations from many instruments, especially over a wide latitude range. Some recent studies [e.g., Bacmeister *et al.*, 1999; Lu *et al.*, 2000; Morris *et al.*, 2000] have used trajectory methods to aid in comparison of ground-based, aircraft, and/or satellite observations. These methods allow comparison of measurements that may be distant by conventional coincidence criteria, but taken in similar air masses. Another way of viewing data referenced to the meteorological conditions under which they were taken is to display them as a function of potential temperature (θ) in coordinates of potential vorticity (PV) [e.g., Schoeberl *et al.*, 1989, 1992; Manney *et al.*, 1994b] or equivalent latitude (EqL, the latitude that would enclose the same area as the corresponding PV contour) [e.g., Butchart and Remsberg, 1986; Schoeberl *et al.*, 1995; Lary *et al.*, 1995; Manney *et al.*, 1999]. This approach is useful for displaying sparse data, such as those from occultation instruments, and for elucidating chemical and transport processes that affect the data under particular meteorological conditions (e.g., in the polar vortex) [e.g., Manney *et al.*, 1999, and references therein]. Because the data are plotted with respect to a meteorological coordinate, these displays can also be helpful in intercomparing data sets with different sampling patterns; limited comparisons of different ozone measurements using this type of coordinate have been made previously by Redaelli *et al.* [1994] (comparing MLS with lidar data) and SPARC [1998] (comparing HALOE and SAGE II data). Particular care must be taken in comparing ozone, even when referenced to meteorological conditions, because the lifetime of ozone in the middle and upper stratosphere is comparable to or shorter than timescales for dynamical changes [e.g., Brasseur and Solomon, 1986], and some chemically driven changes may not correlate well with PV [e.g., Manney *et al.*, 1999].

We use EqL/ θ fields, coincidence criteria augmented by proximity in PV, and reverse trajectory (RT) calculations [Manney *et al.*, 1998, 2000] to compare ozone observations during the ATLAS-3 time period from the seven satellite instruments mentioned above. Each of these methods is used to compare measurements taken in similar (i.e., coincident) air masses, whether or not they are physically coincident. By examining measurements taken under similar meteorological conditions we gain understanding of the consistency between ozone measurements from the seven instruments, and of the dynamical and chemical processes that may result in apparent inconsistencies between observations with different sampling patterns.

¹Jet Propulsion Laboratory, California Institute of Technology, Pasadena, California.

²Visiting at Department of Physics, New Mexico Highlands University, Las Vegas, New Mexico.

³Combustion Research Facility, Sandia National Laboratories, Livermore, California.

⁴Naval Research Laboratory, Washington, D. C., USA.

⁵Physics Department, University of Wuppertal, Wuppertal, Germany.

⁶Center for Atmospheric Sciences, Hampton University, Hampton, Virginia.

⁷Radiation and Aerosols Branch, NASA Langley Research Center, Hampton, Virginia.

2. Data

A summary of the spatial and temporal coverage of available data from ATMOS, SAGE II, POAM II, HALOE, MLS, CRISTA, and MAS during the ATLAS-3 mission is given in Table 1, along with an indication of the approximate vertical resolution and typical precision for the latest data versions. Plate 1 shows examples of the coverage of the various instruments, in relation to the polar vortices, on 2 days during the ATLAS-3 mission. The limb-emission instruments, MLS, CRISTA, and MAS, sample a wide range of latitudes each day. In contrast, ATMOS, SAGE II, HALOE, and POAM II measure limb absorption as the spacecraft is entering or leaving the Earth's shadow; since the latitude of these occultations varies slowly in time (depending on the instrument and orbit geometry), occultation observations are confined to a relatively narrow latitude range during the 9-day period studied. A brief description of the ozone measurements from each instrument, including key references, is given below.

2.1. ATMOS Data

The space-shuttle-borne Atmospheric Trace Molecule Spectroscopy (ATMOS) instrument is a Fourier transform infrared spectrometer that operates in solar occultation mode. ATMOS data have recently been reprocessed with version 3 software (F. W. Irion et al., manuscript in preparation, 2001). ATMOS spectra are recorded with a vertical spacing of ~ 2 km in the lower stratosphere to ~ 4 km in the upper stratosphere; this vertical spacing, combined with the instrument field of view, leads to an effective vertical resolution of $\sim 2\text{-}6$ km [Gunson et al., 1996], with better resolution in the lower than in the upper stratosphere. For each occultation during ATLAS-3 the signal-to-noise ratio was optimized by the use of one of a set of four optical band-pass filters (numbered 3, 4, 9, and 12); ozone was measured in all filters. Filter 4 data are not used here below 30 km because of large uncertainties and biases with respect to the other filters. The version 3 data set shows a number of improvements over version 2, particularly in the upper troposphere and lower stratosphere; agreement in ozone between filters is improved (F. W. Irion et al., manuscript in preparation, 2001). The precision of version 3 ATMOS ozone varies between filters; typically the total random error is $\sim 6\text{-}10\%$ for filters 3, 9, and 12 between about 23 and 40 km, and over 15% at all levels for filter 4. Random errors for filters 3 and 9 increase to near 15% near the stratopause and at ~ 20 km; uncertainties for filters 3, 9, and 12 increase to near 30% around 15 km (where ozone values are low). Preliminary estimates indicate systematic errors from ~ 3 to 9% in the stratosphere. The November 3-12, 1994, ATLAS-3 data have sunrise observations from $\sim 64^\circ$ to 72° S and sunset ob-

servations from $\sim 4^\circ$ to 50° N. More information on ATMOS data can be found at <http://remus.jpl.nasa.gov>.

2.2. SAGE II Data

The SAGE II solar occultation instrument uses radiances at 600 nm to derive ozone profiles. The instrument, earlier versions of the retrieval algorithm, and ozone validation are discussed by Chu et al. [1989], Cunnold et al. [1989], and McCormick et al. [1989]. The previous version of SAGE II data (version 5.96) is discussed extensively by SPARC [1998]. SAGE II data have recently been reprocessed using version 6 retrieval algorithms, which represent a major revision. Information on SAGE II data can be found at <http://www-sage2.larc.nasa.gov>. Version 6 ozone data have ~ 1 km or less vertical resolution, and the precision of the ozone observations is usually less than 1% in the middle stratosphere, increasing to $\sim 2\%$ near the stratopause and tropopause and to higher percentages in regions of very low ozone. A rough estimate, including uncertainty in cross sections and knowledge of spectral response, suggests uncertainties around 2.5% from all systematic sources. SAGE II observations take approximately a month to cover the full range of latitudes sampled (ranging from $\pm 80^\circ$ to $\pm 50^\circ$, depending on season). During ATLAS-3, SAGE II observed from ~ 57 to 72° S, and from ~ 33 to 52° N.

2.3. POAM II Data

POAM II, described by Glaccum et al. [1996], was a visible/near-infrared solar occultation instrument that flew on the Satellite Pour Observation de la Terre (SPOT) 3 spacecraft, and obtained data until the host satellite failed in late 1996. It was designed to measure ozone with a vertical resolution near 1 km in the polar stratosphere and upper troposphere. The POAM II version 5 retrieval algorithm and formal error analysis are discussed by Lumpe et al. [1997], and comparison of version 5 ozone observations with ozonesondes and other satellite instruments are given by Deniel et al. [1997] and Rusch et al. [1997]. Vertical resolution is near 1 km between 20 and 40 km, increasing to ~ 1.5 km at higher and lower altitudes. Precision of version 6 POAM II ozone data is $\sim 2\text{-}5\%$ outside regions of extremely low ozone; estimates of total systematic errors range from ~ 2 to $\sim 5\%$ [Lumpe et al., 1997]. POAM II provided measurements at $\sim 69\text{-}72^\circ$ S and $67\text{-}69^\circ$ N during the time period of the ATLAS-3 mission. Further information and POAM II data are available from <http://opt.nrl.navy.mil/POAM/>.

2.4. HALOE Data

The UARS HALOE instrument [Russell et al., 1993] measures ozone with a broadband radiometer in the $9.6\ \mu\text{m}$

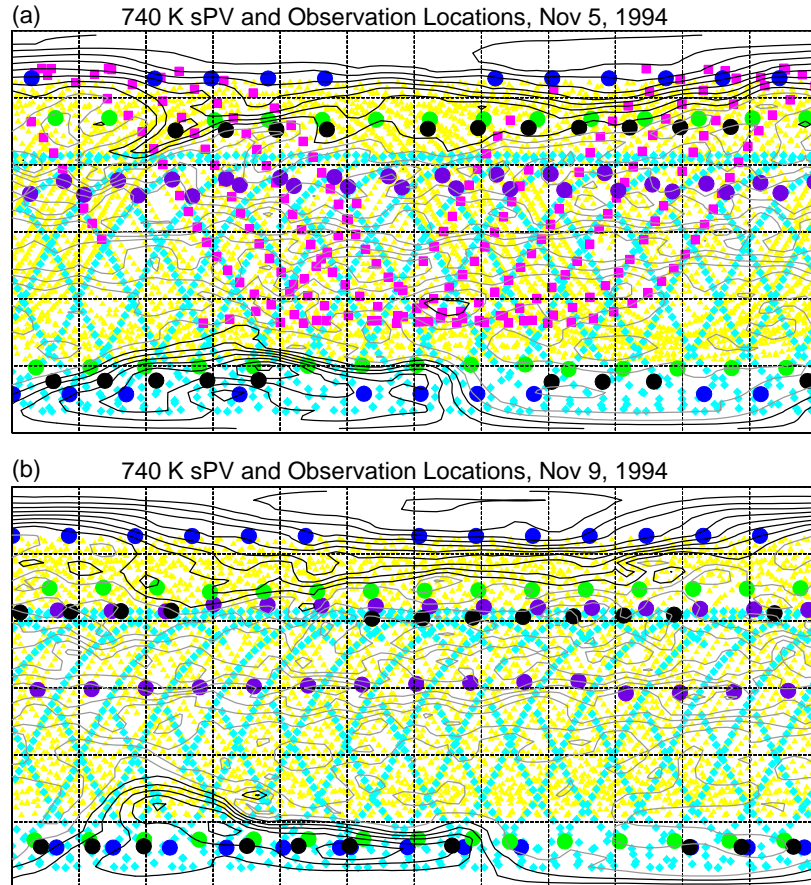


Plate 1. Sampling patterns for ozone observations on (a) November 5 and (b) November 9, 1994, with contours of sPV at 740 K overlaid. Orange triangles show CRISTA observations, cyan diamonds show MLS observations, magenta squares in Plate 1a show MAS observations on November 4, olive circles show POAM II observations, lavender circles show HALOE observations, green circles show SAGE II observations, and black circles show ATMOS observations. The sPV contour interval is $0.2 \times 10^{-4} \text{ s}^{-1}$, with values of $1.2 \times 10^{-4} \text{ s}^{-1}$ and higher in the NH, and $-1.2 \times 10^{-4} \text{ s}^{-1}$ and lower in the SH, in black (representing approximately the polar vortex regions), and intermediate values in grey.

Table 1. Satellite Ozone Observations During November 3-12, 1994

Instrument	Vertical Resolution, ^a km	Precision, ^a %	NH Latitudes, deg N	SH Latitudes, deg S	Dates in November 1994	Data Version
ATMOS	2-6	4-10	4-49	64-72	3-12	3
SAGE II	1	<1-2	33-52	57-72	4-12	6
POAM II	1	2-5	67-69	69-72	4-12	6
HALOE	2	<1-2	0-44	0-10	4-12	19
MLS	4	4-10	0-34	0-80	5-11	5
CRISTA	2-3	2-5	0-67	0-57	4-11	4
MAS	5-7	4-10	0-73	0-39	3-4	20

^aApproximate vertical resolution and precision are as estimated by the instrument teams; the methods used to estimate these vary between instruments.

band, using the solar occultation method. HALOE's 1.6 km instantaneous vertical field of view, combined with the retrieval algorithms and vertical sampling interval of 0.3 km, result in a vertical resolution for ozone of ~2 km. Version 19 HALOE ozone data are used here; these are very similar to version 18. Brühl *et al.* [1996] discuss validation of version 17 ozone data, including estimates of systematic and random errors. Lingenfelter *et al.* [1999] compared version 18 HALOE data with in situ aircraft observations; version 18 HALOE data are compared with version 5.96 SAGE II data by SPARC [1998]. Further information on HALOE data can be found at <http://haloedata.larc.nasa.gov/home.html>. The error estimates provided in the HALOE data files include random components due to noise and altitude dependent quasi-systematic errors due to uncertainties in aerosol corrections. These are typically much less than 1% in the middle and upper stratosphere, increasing to a few percent near the tropopause. These are usually not the dominant error sources for ozone, and systematic errors [Brühl *et al.*, 1996] should be considered when analyzing these data. Estimates of total uncertainty, including these systematic effects, range from about 5-10% in the middle and upper stratosphere, up to around 30% at 100 hPa; in terms of mixing ratio, uncertainties in the lower stratosphere are ~0.3-0.4 ppmv. The HALOE sampling pattern is similar to that of SAGE II. HALOE observed from ~10°S to 44°N during the time of the ATLAS-3 mission.

2.5. MLS Data

The UARS MLS instrument [Barath *et al.*, 1993] has been measuring ozone at 205 GHz in the stratosphere and lower mesosphere since September 1991. Characteristics

and validation of version 3 ozone data are described by Froidevaux *et al.* [1996]. MLS data have recently been reprocessed in version 5. Version 5 data are retrieved on pressure surfaces with ~2.5 km spacing (six levels per decade in pressure), twice as fine a grid as previous versions. More information on MLS data can be found at <http://mls.jpl.nasa.gov>. Preliminary studies indicate that version 5 ozone data agree more closely with correlative data in the lower stratosphere than previous data versions (N. J. Livesey, *et al.*, manuscript in preparation, 2001). The vertical resolution of MLS version 5 ozone is ~3-5 km in the stratosphere. The precision of version 5 ozone is ~4 to 10% between 46 and 1 hPa; precisions increase percentage-wise at lower altitudes, but remain constant at about 0.3 ppmv in the lower stratosphere. Total uncertainties (including possible systematic uncertainties) are ~0.4 ppmv throughout the stratosphere, although this is still being investigated, particularly in the lower stratosphere. In early November 1994, UARS was oriented such that MLS observed from ~80°S to 34°N; MLS obtained good measurements for November 5-11, 1994.

2.6. CRISTA Data

CRISTA measures atmospheric trace gases in a limb-sounding mode using thermal emission at 4-71 μm , with high horizontal resolution obtained by using three telescopes that sense the atmosphere 18° apart. CRISTA operates from a pallet following the space shuttle, and was first flown during ATLAS-3. CRISTA version 1 temperature and trace gas retrievals are described by Riese *et al.* [1999], and an overview of the instrument and observations during ATLAS-3 is given by Offermann *et al.* [1999]. CRISTA's vertical resolution is ~2-3 km. The CRISTA data used here are version 4 retrievals (which, for ozone,

are identical to version 3), which typically have precision near 2% throughout the stratosphere except in regions of very low ozone; systematic errors range from ~ 10 to 15% in the stratosphere. CRISTA operated throughout ATLAS-3, with several different observing modes [Riese et al., 1999]; the data used here are from modes 1 and 2 (stratospheric/mesospheric and stratospheric observations, respectively). CRISTA took measurements throughout the ATLAS-3 mission, with mode 1 and 2 observations on November 4-11, 1994. Further information on CRISTA data can be found at <http://www.crista.uni-wuppertal.de>.

2.7. MAS Data

MAS, which flew on the ATLAS-3 shuttle mission, is a limb-scanning microwave radiometer that measures ozone at 184 GHz. An overview of the MAS measurements on the ATLAS missions is given by Hartmann et al. [1996]. Daehler et al. [1998] discuss validation of the MAS version 20 ozone measurements used here, which are those binned in 128 s batches. The vertical resolution of MAS ozone data is $\sim 5\text{-}7$ km in the 15-50 km altitude range. Typical precision for this altitude range is $\sim 4\text{-}10\%$. Estimates of total error range from 10-15% below 25 km to 4-8% over the rest of the stratosphere. During ATLAS-3, MAS operated only for about 10 hours (due to a computer failure) on November 3-4, 1994, and obtained measurements covering $\sim 40^\circ\text{S}$ to 70°N . Further information can be obtained at <http://www.dfd.dlr.de/info/AUC/MAS/index.html>.

3. Equivalent Latitude/ θ Comparisons

EqL/θ mapping is most useful when trace gases are well-correlated with PV, as is expected for long-lived gases [e.g., Manney et al., 1999] including lower stratospheric ozone. Such mapping may also be useful, as seen below, for shorter-lived gases if those gases remain well-correlated with PV. In this section we explore the comparison of ozone observations in EqL/θ coordinates and the effects of different sampling patterns on these comparisons.

3.1. Methodology

The procedure for mapping ozone into EqL/θ space follows that of Manney et al. [1999]. Scaled PV (sPV, [e.g., Dunkerton and Delisi, 1986; Manney et al., 1994a]) from the Met Office (UKMO) data, interpolated (bilinearly in the horizontal and linearly in $\log\theta$ in the vertical) to the observation locations, is used to grid the data by taking a weighted average of all observations falling within a prescribed distance in PV and $\log\theta$ of each grid point; a Gaussian weighting function is used. The observations are gridded with $0.2 \times 10^{-4} \text{ s}^{-1}$ spacing in sPV in the horizontal

and on 19 levels in the vertical between 380 and 2000 K (~ 15 to 50 km), giving a vertical grid spacing of ~ 2 km. The selection of grid spacing and half width for the weighting function in PV is based on striking a balance, for the instruments with sparse coverage, between reasonable coverage of regions where PV gradients are weak (where a small change in PV would correspond to a large distance, arguing for closer spacing) and not too many empty grid boxes in regions where there is good data coverage but PV gradients are very strong (where very closely spaced PV values would result in many grid boxes with no observations); the sPV half width is $0.1 \times 10^{-4} \text{ s}^{-1}$. For most of the instruments, the half width in θ is also half the size of a grid box. However, for MLS and MAS data, which are reported on grids with larger vertical spacing than that used here, the θ half width is $\sim 20\%$ wider, to provide more uniform coverage of the vertical bins. All data within two half widths in PV and θ of the grid point are included in the average; however, a value is not calculated unless there is at least one observation within one half width of the grid point.

The values averaged at each grid point are also weighted by the estimated retrieval uncertainty provided with each data point (except for CRISTA, where such values are not provided for each observation); these uncertainties typically represent an estimate of precision. A Gaussian weighting function is applied to the uncertainty value from each point that goes into a given average, with the central value at zero uncertainty, so points with smallest errors are weighted most heavily. The error weighting is done by mixing ratio, rather than percent, so as not to misrepresent extremely low ozone values (such as in the Antarctic ozone hole), which may have extremely large percent errors that are very small in absolute value. The error weighting is designed to exclude only extreme outliers: The half width is 0.5 ppmv (so data with very small uncertainties are weighted highly). All data having uncertainties less than 10 ppmv are included (so data with very large uncertainties are included, but are given negligible weight if any values with smaller uncertainties are present).

After gridding in PV/ θ space, EqL is calculated for each PV grid point value, and the fields are interpolated linearly to a uniform EqL grid. The interpolation routine is restricted from filling across large gaps; thus the coverage in the plots represents the actual data coverage.

The precision estimates for each point have been propagated through the gridding (averaging) procedure. The averaging results in random errors values for the gridded fields small enough ($\lesssim 0.1$ ppmv, except at a few points near the edges of the range with error values for the averages up to ~ 0.3 ppmv, for all instruments) that the systematic uncertainties (which are not reduced by averaging) are dominant;

these systematic effects are typically from ~ 2 to 15% depending on the instrument (section 2), with much larger percentages than these in regions of very low ozone.

A measure of the scatter in the values being averaged is obtained by calculating a standard deviation for the points averaged in each grid box, weighted by the squares of their averaging weights. As expected, this scatter is largest in regions where ozone is not well-correlated with PV (section 3.2) and where PV (and ozone) gradients are very strong.

Meteorological conditions during ATLAS-3 are discussed in detail by *Manney et al.* [1999]. The Southern Hemisphere (SH) polar vortex was in the process of its springtime breakup, with a well-defined, but weakened, polar vortex still present in the middle stratosphere (e.g., 840 K) and a relatively strong vortex in the lower stratosphere. Vortex remnants were apparent up to ~ 1300 K [e.g., *Manney et al.*, 1996]. The vortex was shifted far off the pole, and tongues of vortex air were peeled off its edge, while large tongues of low-latitude air were drawn up, either around the vortex or into an anticyclone. The large asymmetry of the SH vortex results in very good EqL/ θ coverage, even for instruments (ATMOS, SAGE II, POAM II) that observed narrow ranges at high latitudes; substantial coverage of both vortex and extravortex conditions by ATMOS, SAGE II, and POAM II can be seen in Plate 1.

In the Northern Hemisphere (NH), the developing polar vortex (the “protovortex”) was shifted off the pole and elongated by a minor warming. *Manney et al.* [2000] discuss in detail the effects of these meteorological conditions on transport, lamination, and filamentation in long-lived trace gases observed by ATMOS during ATLAS-3. Although less disturbed than the decaying SH vortex, there is enough asymmetry in the NH vortex that EqL/ θ mapping substantially increases the coverage (Plate 1). Although NH POAM II data do not physically overlap ATMOS, SAGE II, HALOE, or MLS data (Table 1 and Plate 1), there is significant overlap with ATMOS, SAGE II, and HALOE in EqL/ θ space, and some overlap with MLS.

The validity of EqL/ θ mapping depends also on the relationship between PV and ozone remaining approximately constant throughout the period considered. Over the short (9-day) period studied here, the effects of diabatic descent are sufficiently small that changes in the relationship between PV and ozone are negligible.

3.2. Results

Plate 2 shows EqL/ θ ozone fields during ATLAS-3 from CRISTA, ATMOS, SAGE II, POAM II, HALOE, MLS, and MAS. Plate 3 shows differences in EqL/ θ space between

ozone from CRISTA and each of the other six instruments. Similar plots have been made for MLS (which had best coverage of the SH), ATMOS, and SAGE II (which had substantial EqL/ θ coverage in both hemispheres); although space considerations prohibit showing all of these figures, comparisons of multiple instruments with each of the others facilitate identification of differences between specific instruments. The CRISTA comparisons are shown because CRISTA had the most complete overall coverage of EqL/ θ space. These differences are shown in mixing ratio, as very large percent differences (white overlaid contours) in regions of very low ozone can be misleading.

Ozone is expected to be well-correlated with PV in the lower stratosphere where instantaneous chemical lifetimes are generally long compared to transport timescales, and thus sampling differences should be largely compensated for by the EqL/ θ mapping. Consistent with this expectation, there is very good agreement between all ozone observations below ~ 650 K, usually better than 0.25 ppmv, and always better than 0.5 ppmv except in isolated regions. Although the ozone hole is chemically produced, because extreme ozone depletion took place earlier in the season, and ozone has had a chance to be mixed by transport within the vortex (particularly along PV contours), ozone mixing ratios here are fairly well correlated with PV (i.e., the contours of ozone and PV are the same shape). However, standard deviations at grid points in the ozone hole are $\sim 0.15\text{--}0.3$ ppmv (which is near 100% in some regions), suggesting that these low values may be reaching the limits of the instruments’ precisions.

CRISTA ozone is somewhat higher than ATMOS, SAGE II, POAM II, and MLS in the vortex interior between ~ 500 and 600 K. These differences may be related to remaining inhomogeneities (the presence of which is suggested by results in section 5) in ozone in the vortex interior, as CRISTA SH vortex observations extended less deeply into and were confined to one side of the vortex (e.g., Plate 1). The values for the other four instruments all agree within ~ 0.5 ppmv in this region, and ATMOS, SAGE II, MLS, and CRISTA all agree to within 0.25 ppmv in the rest of the SH ozone hole region, and in the extravortex SH lower stratosphere. While percent differences in the ozone hole are as large as $\sim 50\%$ between CRISTA and MLS, and from $\sim 10\text{--}40\%$ for the other instruments, these represent very small differences in the mixing ratios, and the mixing ratios themselves are near the limits of the instruments’ precisions. ATMOS, SAGE II, POAM II, and MLS ozone mixing ratios are all less than 0.25 ppmv below 420 K in the SH vortex (CRISTA did not have retrieved version 4 data at this altitude). Plate 2 shows that, for each of the instruments (ATMOS, SAGE II, POAM II, MLS, and CRISTA)

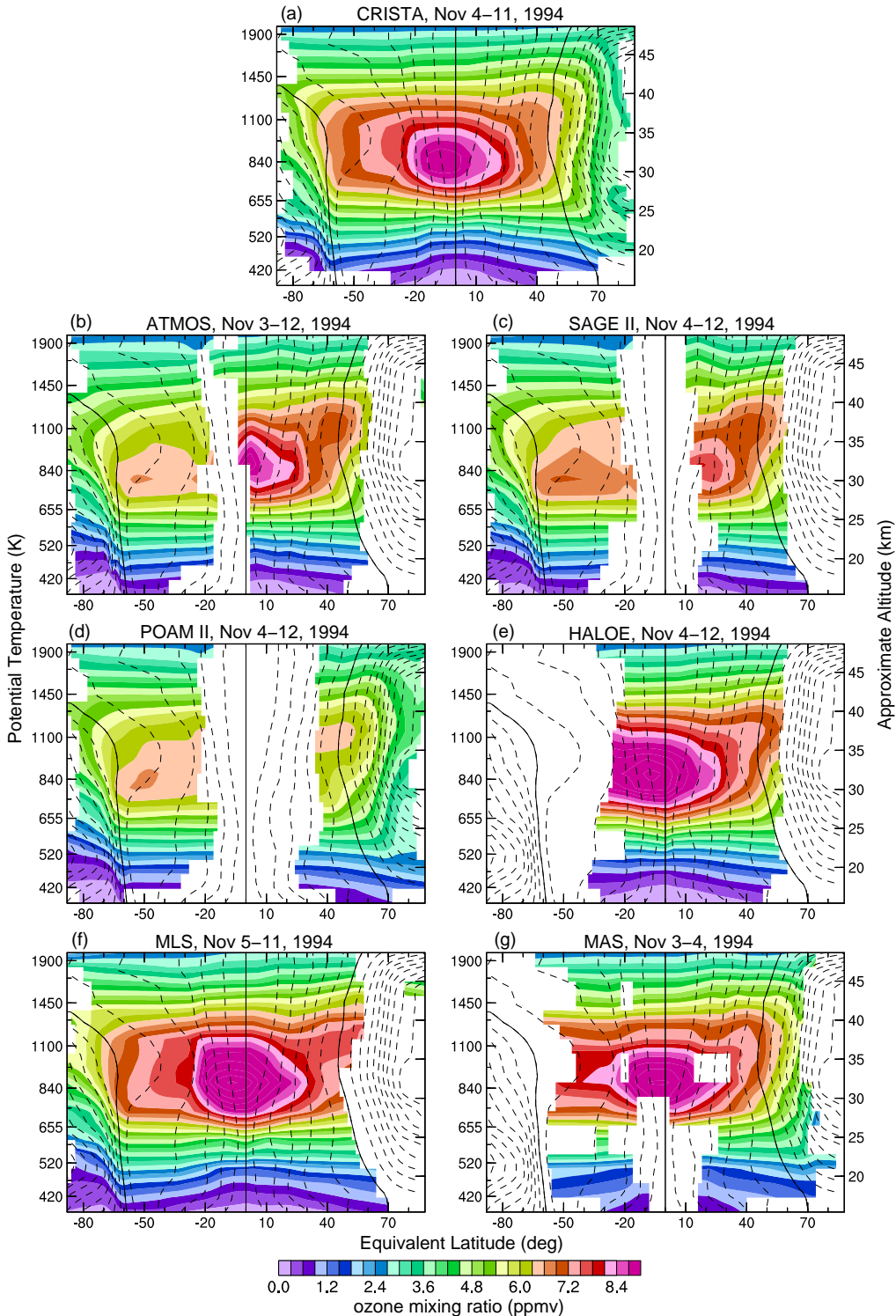


Plate 2. Equivalent latitude (EqL)/θ space fields of ozone from (a) CRISTA, (b) ATMOS, (c) SAGE II, (d) POAM II, (e) HALOE, (f) MLS, and (g) MAS for the indicated days during the ATLAS-3 mission. Fields are shown from 88°S to 88°N EqL. Thin black lines are contours of $|sPV|$, averaged over November 4–11, 1994; the contour interval is $0.2 \times 10^{-4} \text{ s}^{-1}$, with the $1.2 \times 10^{-4} \text{ s}^{-1}$ contour (typically in the vortex edge region) shown as a solid line and the rest as dashed lines; the smallest contour is $0.2 \times 10^{-4} \text{ s}^{-1}$ on either side of the vertical line representing 0° EqL, with values increasing toward the poles. Approximate altitude scale on right side of plots is calculated using the nonlinear formula of Knox [1998].

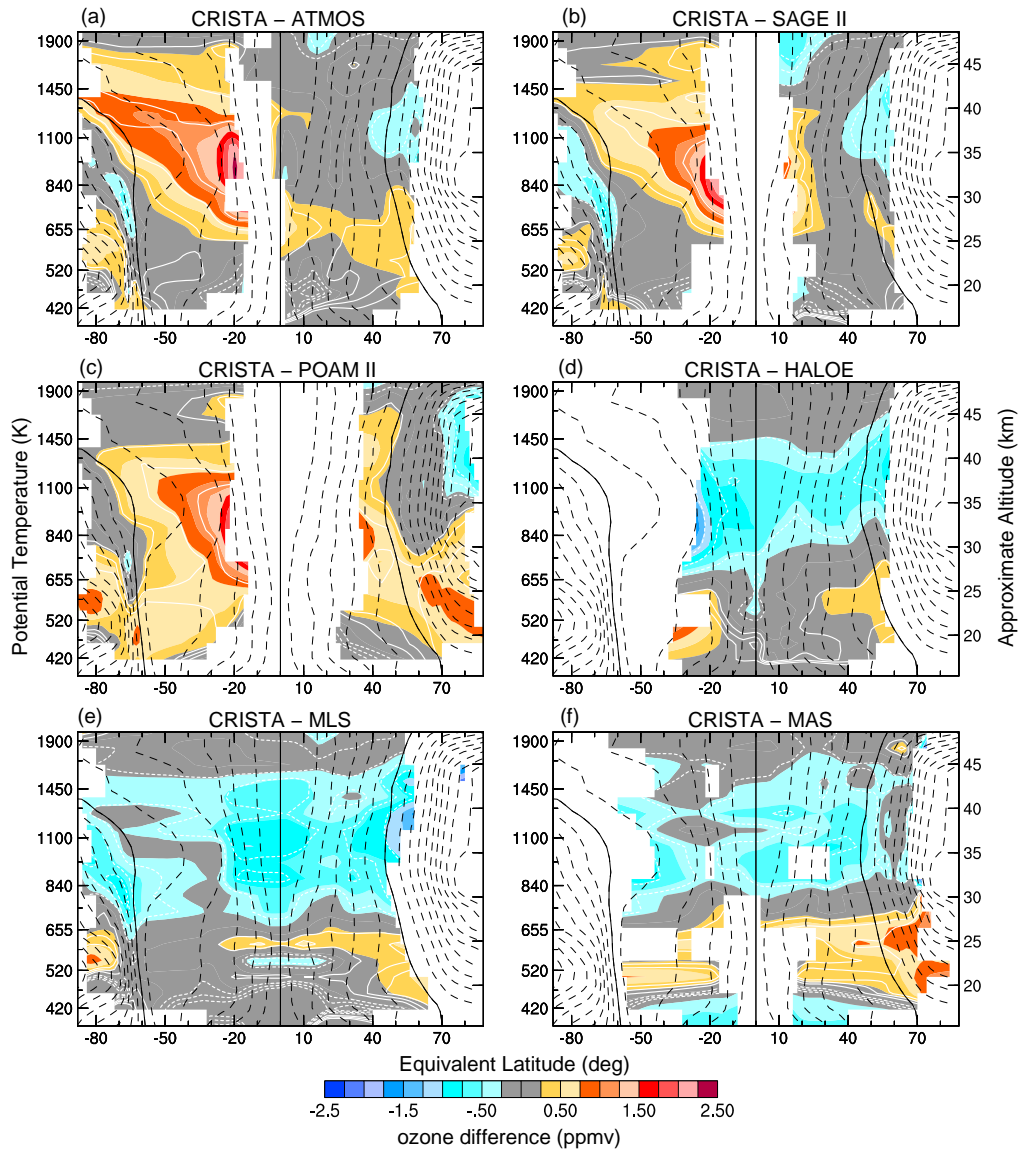


Plate 3. Differences (ppmv) between CRISTA EqL/θ space fields of ozone and EqL/θ fields from (a) ATMOS, (b) SAGE II, (c) POAM II, (d) HALOE, (e) MLS, and (f) MAS. Differences are CRISTA - [instrument], so blue (orange) colors indicate that CRISTA values are smaller (larger) than the other instrument. White contours show -5, -10, and -15% (dashed lines), and 5, 10, and 15% (solid lines) differences. Overlaid thin black lines are sPV, as in Plate 2.

that observed in the SH vortex, there is a slight depression of the ozone contours in the vortex edge region (near $1.2 \times 10^{-4} \text{ s}^{-1}$) between 420 and 520 K; as noted by Manney et al. [1999], this feature is associated with more diabatic descent and less ozone loss along the vortex edge throughout the winter.

Another small region with somewhat larger differences in the lower stratosphere is along the vortex edge in the region of very strong PV (and ozone, Plate 2) gradients, where a very small error in either the PV used in the mapping or the location of the observation could result in large changes in the EqL/θ ozone field. The standard deviations for grid points in this region are larger than typical, indicating more uncertainty in the gridding procedure. Also, some retrievals may not do as well in regions of strong gradients, as the assumption of homogeneity within the field of view may break down. A difference of 0.25 to 0.75 ppmv between CRISTA and POAM II (Plate 3) over the entire SH lower stratosphere (and similar differences between POAM II and MLS, SAGE II, and ATMOS) suggests the possibility of a slight low bias of POAM II data with respect to the other instruments in the SH lower stratosphere, although this difference amounts to only $\sim 10\%$.

CRISTA observations are $\sim 10\text{--}15\%$ higher than both POAM II and MAS in the NH polar lower stratosphere, which may reflect a slight instrument difference, as sampling differences do not provide an obvious explanation. Slightly higher (0.25–0.5 ppmv, $\sim 10\%$) CRISTA than ATMOS and MLS ozone in the NH lower stratosphere between 500 and 650 K is well within the typical systematic uncertainties (which dominate in these plots, section 3.1) of the instruments.

Plates 2 and 3 indicate good agreement (within 0.25 to 0.75 ppmv, or $\sim 5\%$) between ozone from all instruments in the upper stratosphere, above ~ 1450 K, where chemical timescales are much less than dynamical timescales [e.g., Brasseur and Solomon, 1986]. The exception is a small region deep in the protovortex where CRISTA is $\sim 15\text{--}20\%$ lower than POAM II; the standard deviations for CRISTA in this region (at the northern limit of its coverage) are up to ~ 0.8 ppmv, indicating greater uncertainty in the gridded values here. At these levels, the NH protovortex is well developed, and more pole-centered than in the middle stratosphere [Manney et al., 1999, 2000], and temperatures are well-correlated with PV. The SH vortex has broken down at these levels, and there is also a relatively symmetric flow in which temperature and PV are well-correlated. Since the chemical processes that control the short-term evolution of ozone depend strongly on temperature and sunlight, in a situation such as this with relatively symmetric vortices (hence, similar illumination and temperature around a PV contour),

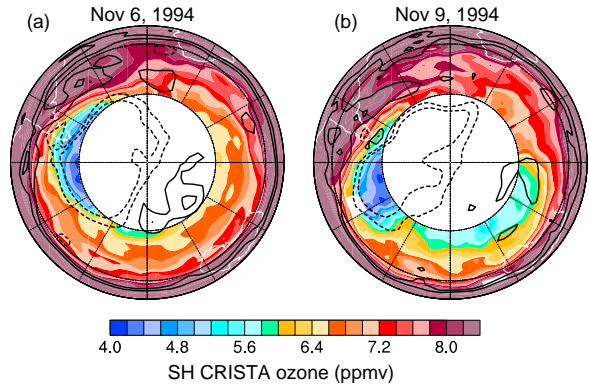


Plate 4. Maps of ozone from CRISTA at 840 K in the SH on (a) November 6, 1994, and (b) November 9, 1994, two days during the ATLAS-3 mission. Contours of $|sPV|$ are overlaid in black; 1.2 and $1.4 \times 10^{-4} \text{ s}^{-1}$ contours are dashed, and 0.6 and $0.8 \times 10^{-4} \text{ s}^{-1}$ contours are solid. The map projection is orthographic, with 0° longitude at the top and 90° E to the right. The domain is from equator to pole, with thin dashed lines at 30° and 60° S.

ozone is still expected to be well-correlated with the vortex.

Much larger differences are seen in the middle stratosphere ($\sim 650\text{--}1450$ K), where the timescales for dynamical and chemical processes are comparable. Because of sampling differences (Plate 1 and Table 1), the latitudes of measurements that go into the mapping for a particular EqL are very different between instruments. As will be seen below, discrepancies between instruments in the middle stratosphere are largely explainable in light of these sampling differences.

In the SH the occultation instruments ATMOS, SAGE II, and POAM II all show values within $\lesssim 10\%$ of each other. The limb-emission instruments, however, MLS, CRISTA, and MAS, all show values 20–30% higher at mid to low EqLs; HALOE observations at low EqL are also over 30% higher than those from the other occultation instruments. ATMOS, SAGE II, and POAM II all sampled a narrow range at high latitudes (Table 1 and Plate 1). As noted by Manney et al. [1999], during ATLAS-3 a “low-ozone pocket” [Manney et al., 1995] had formed in low EqL air drawn up around the polar vortex and into the anticyclone in the middle stratosphere. Low-ozone pockets form when air (initially high in ozone) drawn up from low latitudes is confined in an anticyclone, and ozone subsequently relaxes photochemically to lower values typical of high latitudes [Nair et al., 1998; Morris et al., 1998]. Plate 4 shows maps of 840 K ozone from CRISTA on November 6 and 9, 1994 (compare

with Plate 7 of Manney et al. [1999], which showed similar maps from MLS data; note that the contour values are shifted down by 0.4 ppmv with respect to those shown by Manney et al. [1999] to show a comparable range of colors in mid-latitudes and along the vortex edge). Because CRISTA measured only to $\sim 60^{\circ}$ S, on November 6 it observed only the edge of the low-ozone pocket, which on that date was centered near 70° S; on November 9, CRISTA sampled about the equatorward half of the low-ozone pocket. Most observations from ATMOS, SAGE II, and POAM II at low EqL were in the low-ozone pocket, and thus associated with much lower ozone than observations of low EqL taken at low latitudes (e.g., those from HALOE). MLS and CRISTA fields at mid to low EqL combine observations taken both inside and outside the low-ozone pocket (e.g., Plate 4); the abrupt drop in ozone from tropical values at ~ 20 - 30° EqL seen in Plate 2 for these instruments results from averaging measurements from both inside and outside the low-ozone pocket at sPV from ~ 0.7 to $1.0 \times 10^{-4} \text{ s}^{-1}$. The MAS observations, at $< 40^{\circ}$ S, were well equatorward of the low ozone pocket, giving higher ozone values in ~ 40 - 50° EqL near 800-900 K than CRISTA or MLS (Plates 2 and 3). Consistent with the lack of correlation between PV and ozone in the low-ozone pocket region, both CRISTA and MLS values at grid points in this region have large standard deviations ($\gtrsim 1$ ppmv, up to $\sim 20\%$), and ATMOS, SAGE II, and POAM have larger standard deviations (~ 0.7 ppmv, $\sim 15\%$) than in other parts of the midstratosphere.

MLS values near the mixing ratio peak at ~ 0 - 40° S EqL are ~ 10 - 15% higher than those from CRISTA and 5- 10% higher than those from MAS. Since all three instruments have good coverage of these EqLs, sampling differences do not offer an immediate explanation for these differences.

Differences between instruments in the NH middle stratosphere range between ~ 5 and 15% (Plate 3). NH observations by ATMOS, SAGE II, and HALOE covered similar latitudes (Table 1 and Plate 1), with SAGE II observing at slightly higher latitudes, and HALOE at slightly lower latitudes with better coverage of the tropics, than ATMOS. POAM II observed at much higher latitudes, with no overlap with ATMOS, SAGE II, HALOE, or MLS. CRISTA and MAS have observations throughout the hemisphere, up to $\sim 70^{\circ}$ N. The highest latitudes sampled by ATMOS, SAGE II, and HALOE are in a region of filamentation and mixing of low- and high-latitude air around the protovortex [Manney et al., 2000]. These instruments thus sampled a mixture of air from the protovortex edge region, high-ozone air recently drawn up from the tropics, and air that was drawn up from the tropics earlier. Ozone maps from CRISTA in the middle stratosphere (Plate 5, contour scale is shifted from Plate 4) show a feature resembling a low-ozone pocket. Manney

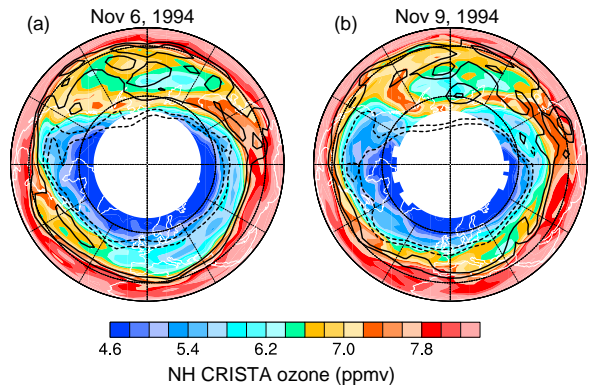


Plate 5. Maps of ozone from CRISTA at 840 K in the NH on (a) November 6, 1994, and (b) November 9, 1994. Contours of $|sPV|$ are overlaid in black; 1.4 and $1.6 \times 10^{-4} \text{ s}^{-1}$ contours are dashed, and 0.8 and $1.0 \times 10^{-4} \text{ s}^{-1}$ contours are solid. The map projection is orthographic, with 0° longitude at the bottom and 90° E to the right. The domain is from equator to pole, with thin dashed lines at 30° and 60° N.

et al. [2000] noted that the ATLAS-3 mission took place during a period with dynamical conditions similar to early winter minor warming events previously reported in December [e.g., Juckes and O'Neill, 1988; Rosier et al., 1994, and references therein]. Although low-ozone pockets have not previously been reported before mid-December [Manney et al., 1995], air drawn up from low latitudes during ATLAS-3 was pulled into the developing anticyclone and confined there for several days [e.g., Manney et al., 1999, 2000], creating the conditions under which low ozone pockets are expected. Examination of profiles from CRISTA and several of the other instruments shows the characteristic “bite” out of the ozone profiles in the middle stratosphere that is associated with low-ozone pockets [Manney et al., 1995].

In the NH all instruments except POAM II and MLS had good coverage of midlatitudes (~ 30 - 50° N); all except SAGE II and POAM II had some coverage of the tropics. That SAGE II has lower ozone than CRISTA at the lowest EqLs it sampled (Plate 3b) is because SAGE II sampled low PV ($sPV = 0.4$ - $0.8 \times 10^{-4} \text{ s}^{-1}$) primarily in the anticyclone where the low-ozone pocket formed. Conversely, MLS shows higher values than CRISTA at all EqLs sampled (Plate 3d) because it sampled low PV only in the tropics, whereas CRISTA sampled low PV both in the tropics and in the low-ozone pocket. CRISTA sampling resulted in higher standard deviations (~ 0.7 ppmv, $\sim 15\%$) in this region. Somewhat lower ozone from POAM II (Plate 3c) at mid-EqLs is expected because those observations (near

68°N) sampled air in the protovortex edge region that had been well within the vortex, where ozone was lower. Tropical tongues drawn up around the vortex did not extend past 60°N, and POAM II would not have sampled them. ATMOS, SAGE II, HALOE, CRISTA, and MAS observations near the protovortex edge, however, include observations in such tropical tongues. It is unclear whether the ~10% differences between CRISTA and HALOE are related to the sampling, although HALOE observations were concentrated more in the tropics and may thus reflect an average weighted more toward the tropics and higher ozone. Plate 1 shows that MAS sampling in NH midlatitudes outside the protovortex was primarily in regions away from the low-ozone pocket, whereas that of CRISTA was uniform in longitude; this difference may account for ~5-8% higher values seen by MAS.

Agreement in EqL/θ-mapped ozone is very good among all seven instruments in the upper stratosphere (where chemistry dominates) and in the lower stratosphere (where dynamics dominates). Differences in the middle stratosphere, where chemical and dynamical timescales are comparable appear to be largely explainable by differences in the sampling. To examine in more detail the agreement between instruments, and to verify some of the sampling effects discussed above, we look below at comparisons of individual profiles that were observed in similar air masses.

4. Profile Comparisons

To compare observations taken under similar conditions, we chose profiles that are as closely coincident as possible in PV. Because of the different sampling patterns for the instruments considered, criteria for coincidence in time and longitude are relaxed if necessary to find close coincidence in PV and in latitude (since solar illumination is an important factor in the evolution of ozone). We have thus compared values only for coincident or nearly coincident latitudes, but which may or may not have close coincidence in longitude and time.

4.1. Southern Hemisphere

Table 2 lists the profiles compared in the SH. ATMOS, SAGE II, POAM II, and MLS observed high latitudes (~62–73°S) in the SH; Plate 6 shows these profile comparisons. Both vortex and vortex edge profiles agree to within 0.5 ppmv for all four instruments in most places, which is better than 10% except in the lower stratosphere. ATMOS, SAGE II, and POAM II vortex profiles all show evidence of a narrow lamina near 700 K; MLS may not fully resolve such a feature because of its coarser vertical resolution, although the profile does show a shoulder here. SAGE II and MLS

profiles show a lamina in the lower stratosphere, just above 400 K, that is not apparent in ATMOS or POAM II profiles, possibly due to the different sampling locations. The vortex edge profiles are located so that the profile is within the vortex below ~600 K, and outside the vortex above that level. All instrument profiles show very low ozone (<0.5 ppmv) in the lower stratosphere, comparable to values for the profile deeper inside the vortex; since these values are so low, percent differences are large, even though the four profiles all agree to within ~0.3 ppmv, and SAGE II, ATMOS, and POAM II to within ~0.1 ppmv. Just below the mixing ratio peak, SAGE II shows vortex edge values over 1 ppmv (~25%) higher than the other instruments, and above the mixing ratio peak ATMOS shows values nearly 1 ppmv (~15%) lower; larger difference around the mixing ratio peak, where vertical ozone gradients are very steep (especially just below the peak), may result from differences in vertical resolution and altitude or pressure registration in the retrievals.

The profiles outside the vortex show some variation over about 650–1400 K, although the largest differences are still usually $\lesssim 10\%$. The area outside the vortex at high latitudes includes the low-ozone pocket and the entrance region where low-latitude ozone is first drawn up into the anticyclone. Between these two regions there are strong ozone gradients that are not well correlated with PV: air in the entrance region at a given PV value will have much higher ozone than that in the low-ozone pocket at the same PV (see, e.g., Plate 4). For these profiles (bottom panels of Plate 6) a close match in the longitude was not possible while simultaneously matching PV and latitude (Table 2). The nearly 1 ppmv difference (although only ~10–12%) seen between the SAGE II and POAM II profiles in the lower left panel of Plate 6 results from the POAM II profile being at a longitude closer to the low-ozone pocket than the SAGE II profile. Although the ATMOS and MLS profiles are closely matched in all criteria, the MLS profile is nonetheless nearly 1 ppmv higher between ~1000 and 1500 K.

All of the low-ozone pocket profiles (second from bottom row in Plate 6) are toward the edges of that region, with the MLS profile being slightly closer to the center than the other three. MLS is again a bit higher than ATMOS, SAGE II, and POAM II in the middle stratosphere. All profiles in the low-ozone pocket region show a truncated peak, with the ATMOS, MLS, and SAGE II profiles showing a notch in the profile just above 1000 K, as is characteristic of the low-ozone pocket region [Manney et al., 1995].

CRISTA observed up to ~60°S during ATLAS-3, and MAS up to ~40°S. Plate 7 shows comparisons of CRISTA and MLS observations in the vortex and low-ozone pocket, and CRISTA, MLS, and MAS observations in midlatitudes.

Table 2. SH Ozone Profile Comparisons

Instrument	Longitude	Latitude	Date
<i>High-Latitude Profiles (62-73°S), Plate 6</i>			
<i>Inside Vortex</i>			
ATMOS	284.1	-67.8	Nov 6
SAGE II	283.1	-62.2	Nov 6
POAM II	286.7	-72.5	Nov 6
MLS	280.1	-69.4	Nov 6
<i>Vortex Edge</i>			
ATMOS	335.5	-72.1	Nov 11
SAGE II	335.0	-71.1	Nov 12
POAM II	336.4	-70.9	Nov 10
MLS	332.3	-73.0	Nov 11
<i>Low-Ozone Pocket</i>			
ATMOS	183.6	-71.8	Nov 10
SAGE II	182.3	-69.4	Nov 10
POAM II	174.5	-71.4	Nov 9 ^a
MLS	178.5	-68.2	Nov 10
<i>Outside Vortex</i>			
ATMOS	71.2	-69.4	Nov 7
SAGE II	57.8	-65.3	Nov 7
POAM II	88.7	-72.0	Nov 7
MLS	69.8	-70.6	Nov 7
<i>Midlatitude Profiles (39-58°S), Plate 7</i>			
<i>Inside Vortex</i>			
MLS	249.9	-57.4	Nov 9 ^a
CRISTA	251.7	-56.9	Nov 9 ^a
<i>Low-Ozone Pocket</i>			
MLS	151.6	-56.3	Nov 9 ^a
CRISTA	150.9	-55.2	Nov 9 ^a
<i>Outside Vortex</i>			
MLS	58.9	-39.4	Nov 5 ^b
CRISTA	57.8	-40.0	Nov 5 ^b
MAS	49.0	-39.8	Nov 4 ^b

^aThese observation locations are represented in Plate 1b.^bThese observation locations are represented in Plate 1a.

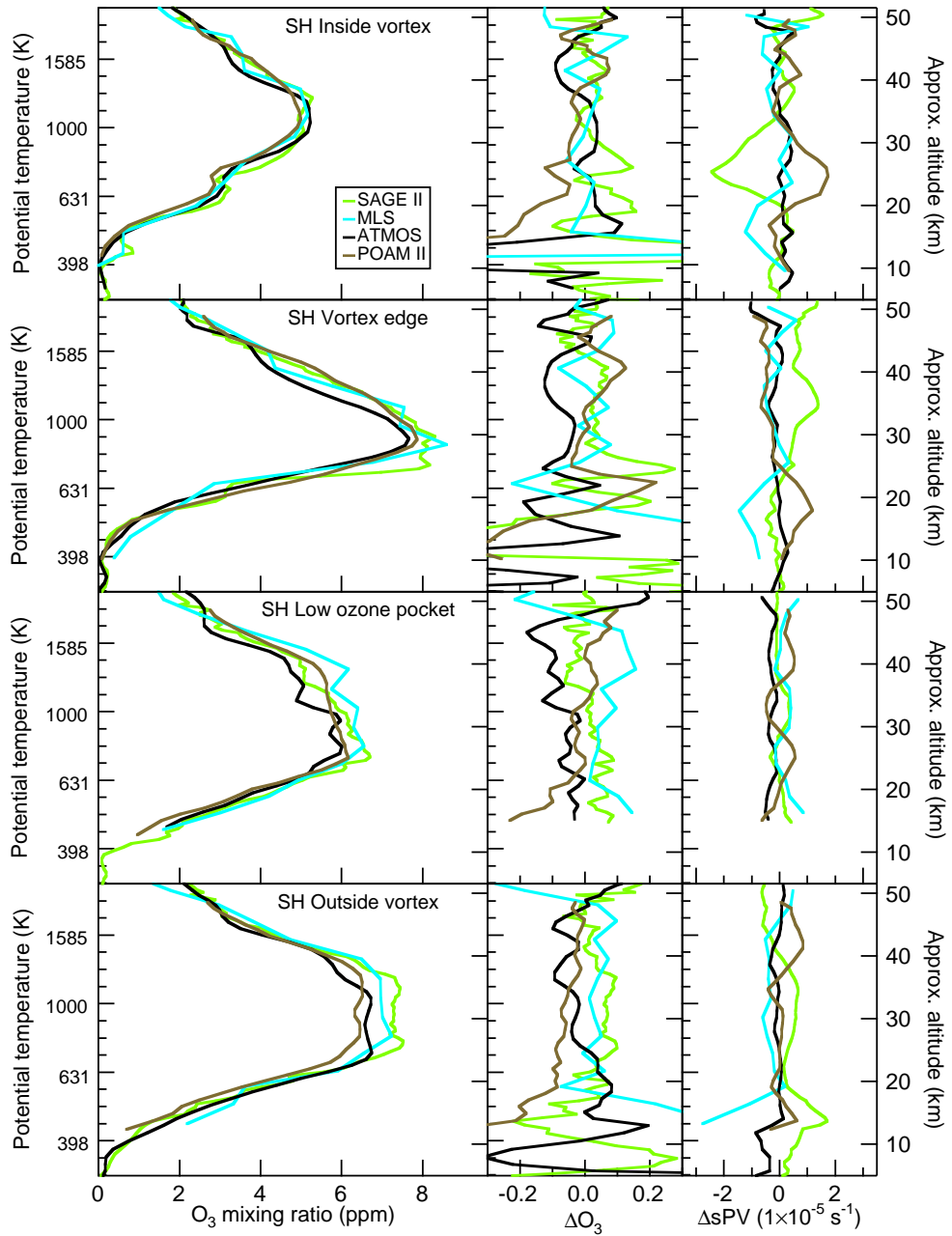


Plate 6. Profile comparisons for instruments that observed high latitudes in the SH ($\sim 65\text{--}75^\circ\text{S}$), for ATMOS (black), SAGE II (green), POAM II (olive), and MLS (cyan). Left panels show ozone mixing ratio (ppmv), middle panels show fractional ozone differences from the average, and right panels show sPV differences from the average (multiplied by 10 from the unit of 10^{-4} s^{-1} used elsewhere in the paper) at the locations of the observations. Note that fractional ozone differences in very low ozone regions may be very large without indicating poor agreement in ozone values.

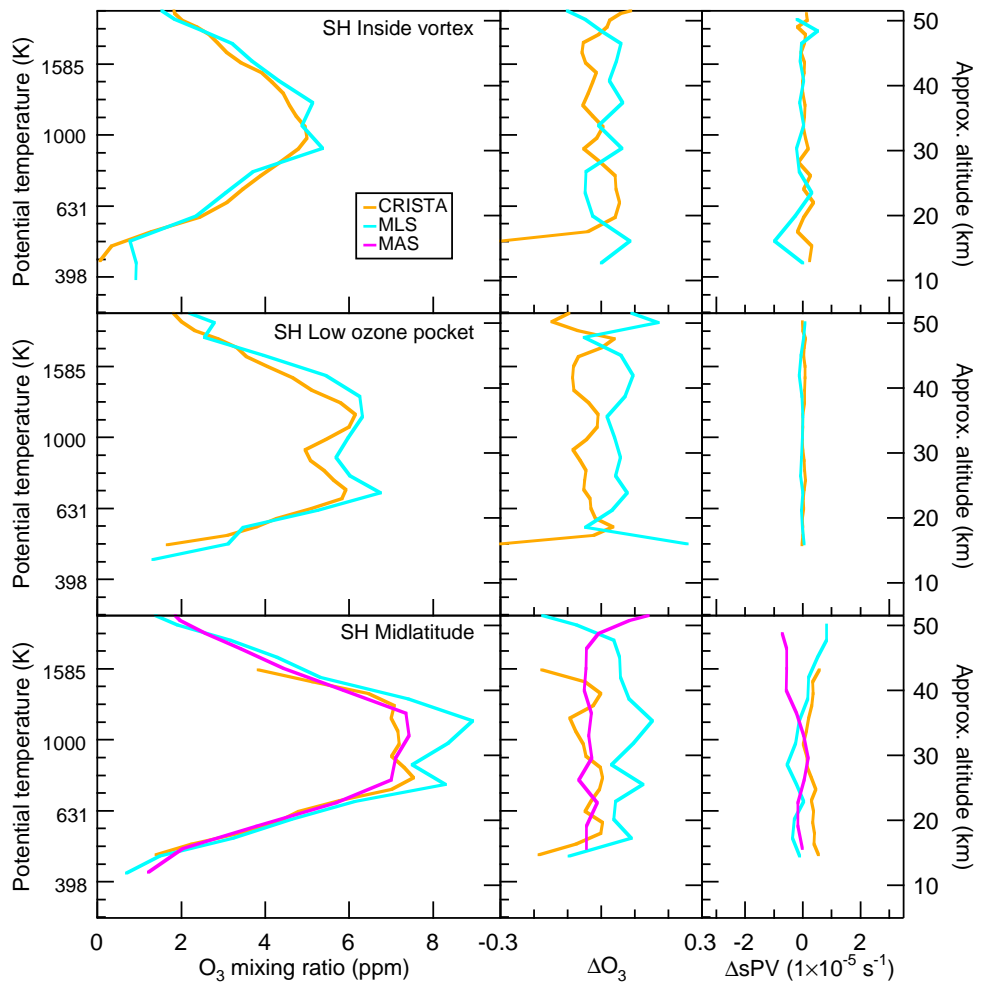


Plate 7. Profile comparisons for mid to high latitudes in the SH ($\sim 40\text{--}60^\circ\text{S}$), for CRISTA (orange), MLS (cyan), and MAS (magenta, midlatitude only). Left panels show ozone mixing ratio (ppmv), middle panels show fractional ozone differences from the average, and right panels show sPV differences from the average.

Because CRISTA and, to a lesser degree MLS and MAS, had relatively dense coverage, closer matches in longitude and time were possible for these comparisons (Table 2). The CRISTA and MLS vortex profiles (top panels) agree well, within 10%, with MLS showing slightly higher values (but well within the uncertainties of the two instruments) in the middle stratosphere, and diverging below ~ 450 K, where uncertainties become very large for both instruments. It was possible to match CRISTA and MLS profiles near the center of the low-ozone pocket (near 150° E) on the same day. Both CRISTA and MLS profiles in the low-ozone pocket (middle panels) show the deep bite out of the profile that is characteristic of this phenomenon. MLS ozone is higher than CRISTA ozone by $\sim 0.5\text{--}0.8$ ppmv (less than 10%) in the middle stratosphere.

The profile comparison outside the vortex near 40° S shows a larger difference (close to 20%) between MLS and CRISTA near the mixing ratio peak, although all coincidence criteria are closely matched between these two profiles (Table 2). The CRISTA and MAS profiles in this case match well (to better than 10%) even in the middle stratosphere, and those from all three instruments match well in the upper and lower stratosphere.

4.2. Northern Hemisphere

Table 3 shows the profiles compared in the NH. Five of the seven instruments (excluding POAM II and MLS) had observations in northern midlatitudes, both inside and outside the protovortex edge region, and four of these five instruments, and MLS, observed the NH tropics; the comparison includes SAGE II observations from a few days after the end of the ATLAS-3 mission when SAGE II observed the tropics. Plate 8 shows these comparisons. All five instruments show excellent agreement throughout the stratosphere in the protovortex and protovortex edge region (top two rows in Plate 8), usually to better than 0.5 ppmv ($\lesssim 10\%$ except in very low ozone regions). The third row of panels in Plate 8 shows measurements distinctly outside, but still near, the protovortex edge region, where ozone and PV gradients are very strong (e.g., Plate 5). Greater variations ($\sim 15\%$) here may result from comparing samples at different longitudes (Table 3) and with greater PV variations (right panel, third row); however, most differences are still within ~ 0.7 ppmv, generally less than the combined total uncertainties of the various instruments.

The three midlatitude profiles (top three rows, Plate 8) are ones for which Manney et al. [2000] showed laminae in ATMOS long-lived trace gases; ATMOS ozone profiles show corresponding laminae. In cases where the longitudes are near those for ATMOS, the profiles from other instruments show similar laminae (e.g., the SAGE II, HALOE,

and CRISTA profiles in the top two rows; all profiles except that from MAS in the third row). In some cases, similar laminae in multiple instruments' observations occurred even when the observations were several days apart, demonstrating the ubiquity of laminae in the regions preferred for their development [Manney et al., 2000].

The six instruments' profiles compared in the tropics (Plate 8, bottom panels) all agree to within 10–12%. The CRISTA profile is nearly 1 ppmv ($\sim 12\%$) lower than the others just below the ozone mixing ratio peak, and the MLS profile shows abrupt changes at a couple of individual levels. Plates 2 and 3 also showed CRISTA to have somewhat lower ozone (0.5 to 1.0 ppmv) in the middle stratosphere tropics ($\pm 20^{\circ}$ EqL) than HALOE, MLS, and MAS (the other instruments with good tropical coverage), which could not be explained by sampling differences. Although percent differences are large below ~ 600 K, all lower stratospheric tropical profiles are within 0.5 ppmv of each other down to ~ 400 K.

CRISTA, MAS, and POAM II all made measurements near $65\text{--}70^{\circ}$ N (Plate 9) inside the protovortex and near its edge. These profiles all agree to within 10%, with the small differences seen being generally consistent with the differences in the PV of the observations. The POAM II protovortex edge profile has slightly lower ozone than the CRISTA and MAS profiles just below the mixing ratio peak at altitudes where it is also at slightly higher PV. The CRISTA observation inside the protovortex (which has slightly higher PV in the upper and lower stratosphere) has correspondingly lower ozone in the upper stratosphere and higher ozone in the lower stratosphere than the POAM II and MAS profiles. All three instruments' profiles show laminae near 600 K along the protovortex edge and near 550 K inside the protovortex. Agreement is somewhat worse (up to $\sim 20\%$ differences) at and below the level of the lamina inside the protovortex, probably because of differences in sampling locations of a localized feature.

The overall agreement between profiles from all instruments that could be compared, at latitudes and PV values covering most of the globe and a wide variety of meteorological conditions, is remarkably good. The most substantial differences (no more than $\sim 15\%$ outside regions of very low ozone) that are not immediately explicable by variations in sampling are slightly higher values seen by MLS than several other instruments in some SH extravortex profiles in the middle stratosphere, and lower values seen in the midstratosphere in the CRISTA tropical profile than in the other instruments' profiles. A number of profiles examined show laminae that appear in several instruments' observations when those observations are sufficiently closely coincident. In the next section we examine the origins of some

Table 3. NH Ozone Profile Comparisons

Instrument	Longitude	Latitude	Date
<i>Midlatitude and Tropical Profiles (9-50°N), Plate 8</i>			
<i>Protovortex Edge</i>			
ATMOS	275.8	45.5	Nov 5 ^a
SAGE II	292.8	45.5	Nov 8
HALOE	286.3	44.3	Nov 12
CRISTA	267.6	45.6	Nov 5 ^a
MAS	238.2	44.8	Nov 4 ^a
<i>Protovortex</i>			
ATMOS	252.2	42.7	Nov 6
SAGE II	244.4	43.0	Nov 10
HALOE	240.5	42.6	Nov 12
CRISTA	258.6	42.9	Nov 5 ^a
MAS	42.9	49.9	Nov 4 ^a
<i>Outside Protovortex</i>			
ATMOS	251.4	34.5	Nov 6
SAGE II	268.6	33.4	Nov 10
HALOE	248.8	34.2	Nov 12
CRISTA	349.3	42.7	Nov 9 ^b
MAS	194.1	42.1	Nov 4 ^a
<i>Tropics</i>			
ATMOS	253.4	10.0	Nov 12
SAGE II	151.9	9.5	Nov 16
HALOE	150.0	10.2	Nov 7
MLS	221.9	9.8	Nov 11
CRISTA	242.7	9.6	Nov 5 ^a
MAS	258.8	9.1	Nov 4 ^a
<i>High-Latitude Profiles (65-72°N), Plate 9</i>			
<i>Protovortex Edge</i>			
POAM II	167.5	68.5	Nov 6
CRISTA	173.0	66.9	Nov 5 ^a
MAS	156.8	65.3	Nov 4 ^a
<i>Protovortex</i>			
POAM II	129.7	69.0	Nov 3
CRISTA	83.7	65.1	Nov 5 ^a
MAS	139.1	72.0	Nov 4 ^a

^aThese observation locations are represented in Plate 1a.^bThese observation locations are represented in Plate 1b.

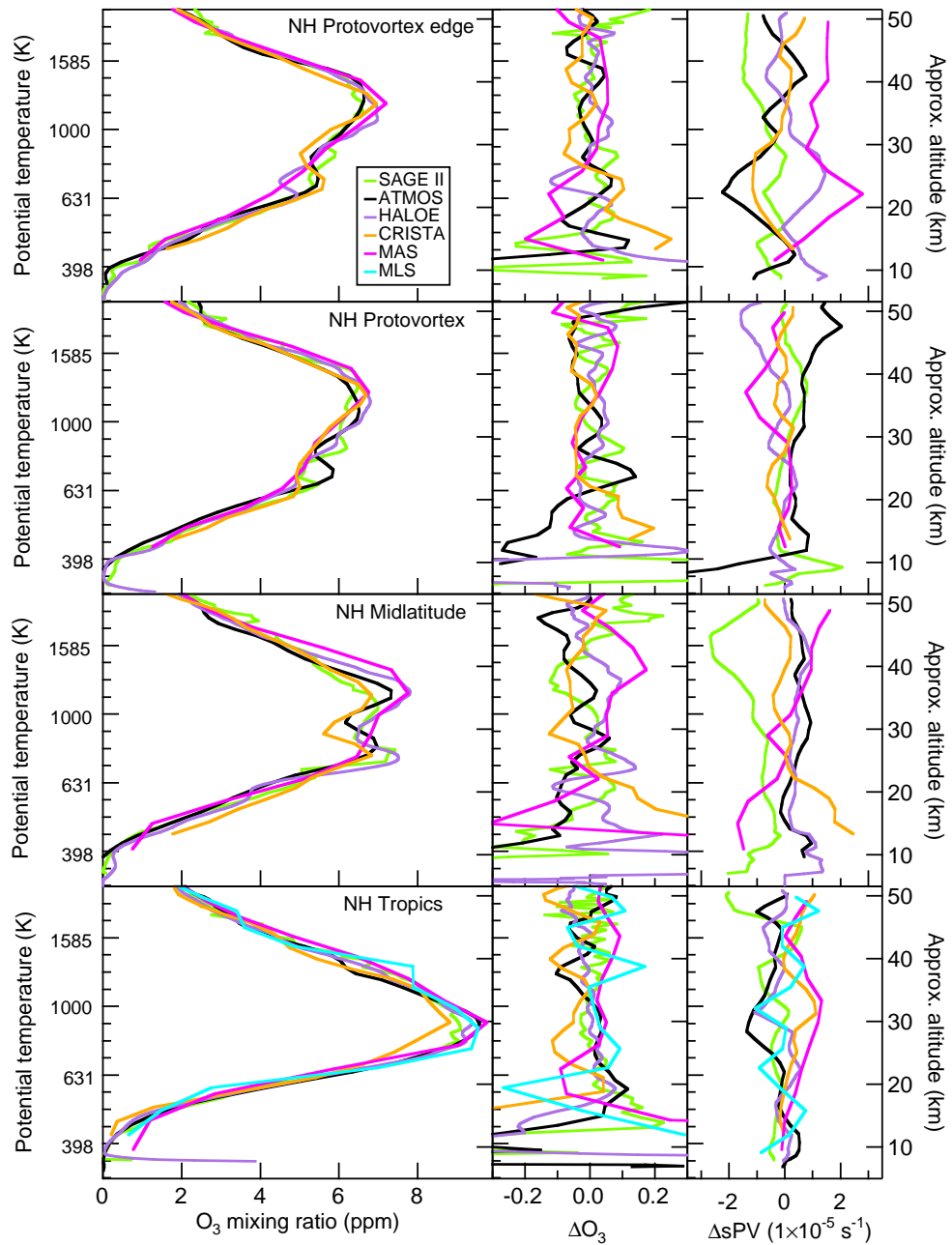


Plate 8. Profile comparisons for midlatitudes and tropics in the NH ($\sim 10\text{--}50^\circ\text{N}$), for ATMOS (black), SAGE II (green), HALOE (lavender), CRISTA (orange), MAS (magenta), and MLS (cyan, tropics only). Left panels show ozone mixing ratio (ppmv), middle panels show fractional ozone differences from the average, and right panels show sPV differences from the average.

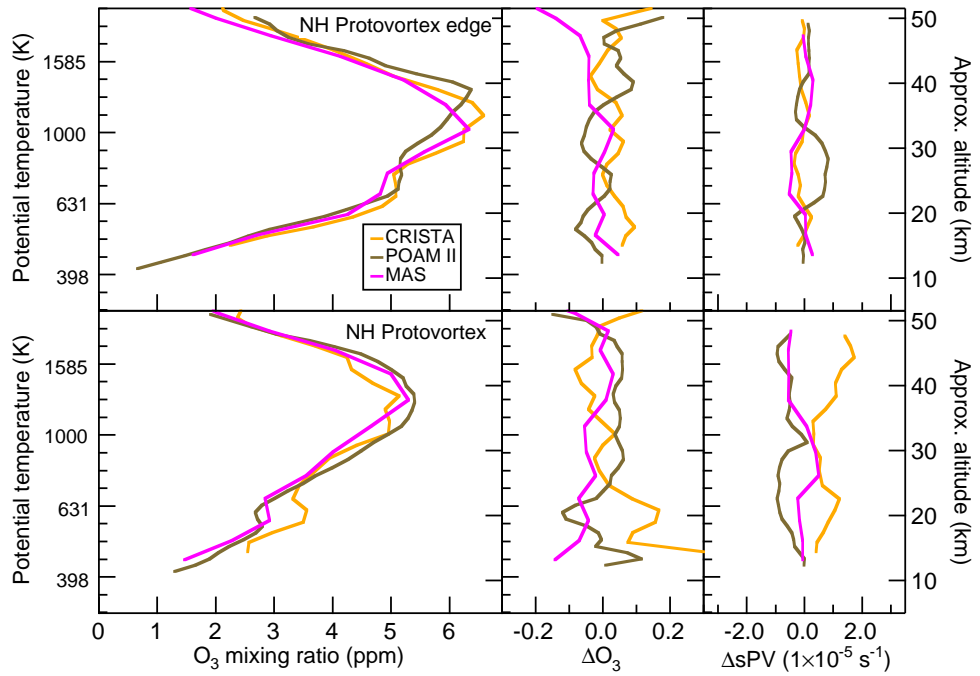


Plate 9. Profile comparisons for high latitudes in the NH ($\sim 60\text{--}70^\circ\text{N}$), for POAM II (olive), CRISTA (orange), and MAS (magenta). Left panels show ozone mixing ratio (ppmv), middle panels show fractional ozone differences from the average, and right panels show sPV differences from the average.

of these small-scale features.

5. Origins of Small-Scale Structure

Manney et al. [2000] used the reverse trajectory (RT) model described below to show that laminae in ATMOS long-lived trace gas profiles arose from chaotic advection by the large-scale wind fields along (both inside and outside) the protovortex edge in the NH during ATLAS-3. As noted above, closely coincident measurements from several instruments often show similar laminae, providing evidence of an atmospheric origin for such features, and suggesting detailed agreement between ozone observations from different instruments. Here we examine the origins of some laminae seen in the ozone profiles compared above to detail the structures they are manifestations of and to confirm their atmospheric origins.

5.1. Trajectory Calculations

The RT calculations, based on the technique developed by *Sutton et al.* [1994], are described in detail by *Manney et al.* [1998, 2000]. High-resolution profiles are obtained at measurement locations on 100 isentropic surfaces equally spaced in $\log\theta$ between 380 and 2000 K (vertical spacing ~ 350 -400 m) from the average of RT calculations for all parcels placed in an 11 by 11 array centered at the measurement location in a 2° longitude by 1° latitude box (~ 100 km per side at midlatitudes). High-resolution RT maps are made on selected isentropic surfaces (chosen from the 100 levels on which the RT profiles are constructed) on an ~ 80 by 80 km equal area grid, interpolated to 0.8° latitude by 1.8° longitude for plotting. All RT calculations are for 7–8 days, initialized at the nearest half-hour (the trajectory time step) to the observation time. This time interval is sufficient to capture laminae of vertical extent greater than ~ 1 km [*Manney et al.*, 1998].

As in the work of *Manney et al.* [2000], the primary initialization data used in the RT calculations are reconstructed (“RC” initialization) from the EqL/ θ fields for the instrument in question, using UKMO PV for the appropriate initialization time (the earliest point of the back trajectory calculation, 7–8 days prior to the ozone observations). To test the sensitivity to the initialization field, calculations were also initialized with the EqL/ θ fields for other instruments, and with an EqL/ θ “climatology” of ozone derived from MLS data (similar to those for long-lived tracers described by *Manney et al.* [1999]).

5.2. Results

Manney et al. [2000] showed that laminae in N_2O , CH_4 , and H_2O measured by ATMOS in profiles corresponding to

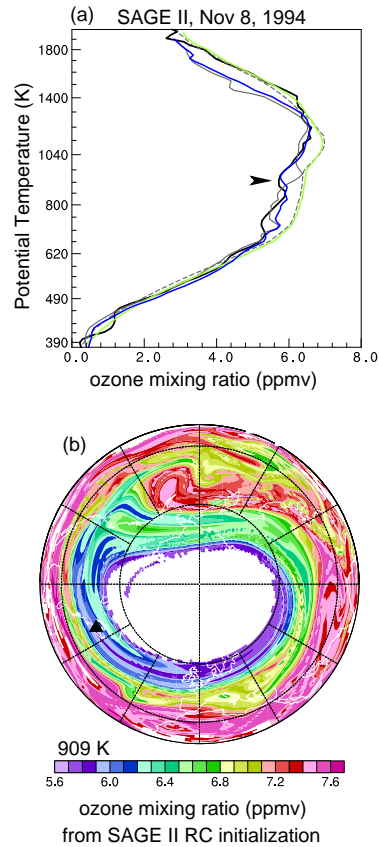


Plate 10. (a) Ozone (ppmv) profiles from SAGE II (black), from RC SAGE II EqL/ θ fields at the observation location (green), from RC ATMOS fields (dashed grey), from RT calculations initialized with SAGE II RC data (blue), and from RT calculations initialized with ATMOS RC data (solid grey). Arrow shows approximate level of map shown in Plate 10b. (b) RT map of ozone at 909 K initialized with RC SAGE II data. The map projection is orthographic, with 0° longitude at the bottom and 90°E to the right; the domain is from equator to pole, with thin dashed lines at 30° and 60°N ; the black triangle shows the location of the SAGE II profile in Plate 10a.

the ozone profiles shown in the top three rows of Plate 8 arose from filamentation in and around the protovortex, or from multiple crossings of the vortex edge at several levels. Consistent with these results, RT calculations reproduce similar laminae corresponding to those in the ATMOS ozone profiles shown in Plate 8. Except where the longitude of observations is very different, other instruments show corresponding laminae. We show below similar origins for some laminae seen in other instruments’ observations.

The origin of a small lamina near 900 K in the SAGE II profile in the top left panel of Plate 8 is shown in Plate 10. The blue line in Plate 10a shows that RT calculations using the SAGE II RC field (Plate 2c) closely reproduce a small depression in ozone near 900 K in the SAGE II profile. RT calculations initialized with the ATMOS RC field (Plate 2b), however, do not reproduce this feature. Examination of RT maps at several levels (e.g., Plate 10b) shows that the laminae from \sim 900–930 K in SAGE II arose from sampling alternately in narrow filaments of higher and lower ozone within the protovortex. That they are better reproduced using the SAGE II initialization suggests that they arise from detailed structure that is not present in the ATMOS EqL/ θ field.

Plate 11 shows similar calculations for the HALOE profile in the top left panel of Plate 8. In contrast to the above case, RT calculations from the ATMOS RC initialization were more successful at reproducing the lamina near 740 K than were RT calculations initialized with the HALOE RC field (Plate 2e). Plate 11b shows that this HALOE profile was near the poleward edge of the ATMOS EqL/ θ coverage (it was, in fact, even closer to the edge of the HALOE coverage). Since ATMOS measured higher geographical latitudes than HALOE (Table 1), these EqLs are more fully and accurately covered in the ATMOS data; also, examination of the positions of the parcels used in the RT calculations at initialization time shows that at several levels near this lamina, parcels were in a region not covered by the HALOE RC field; thus the HALOE RT profile is interpolated between some levels in this altitude range. Plate 11b indicates that the lamina arose from sampling interwoven filaments with higher and lower ozone along the protovortex edge.

Laminae corresponding to those seen in POAM II, CRISTA, and MAS profiles at high latitudes (Plate 9) are apparent in RT calculations using the instruments' EqL/ θ ozone fields for initialization, although there are gaps where parcels came from regions with poor/no EqL/ θ coverage at the high EqL end of the instruments' coverage. RT calculations using the MLS-based climatology, with complete EqL/ θ coverage, reproduced more completely the ozone maxima near 580 K in all three instruments' profiles. Plate 12 indicates that the lamina in the POAM II data arose from sampling a filament of higher ozone well inside the protovortex. Many other such serrations are apparent in Plate 12 in the vortex interior, and the laminae in CRISTA and MAS profiles resulted from sampling such features.

The ATMOS, SAGE II, and POAM II profiles in the Antarctic vortex also showed laminae between 650 and 750 K (Plate 6, top row); MLS profiles coincident with these show a corresponding shoulder. RT calculations for each of these profiles show evidence of laminae, but they do not match very closely the exact altitudes and shapes of the lam-

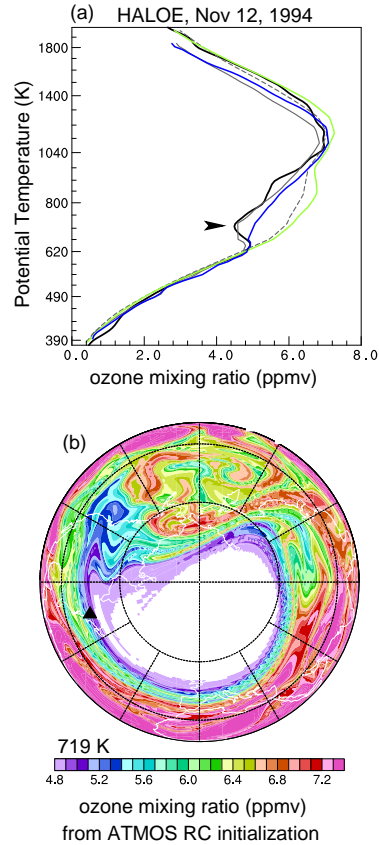


Plate 11. (a) Ozone (ppmv) profiles from HALOE (black), from RC HALOE EqL/ θ fields at the observation location (green), from RC ATMOS fields (dashed grey), from RT calculations initialized with HALOE RC data (blue), and from RT calculations initialized with ATMOS RC data (solid grey). Arrow shows approximate level of map shown in Plate 11b. (b) RT map of ozone at 719 K initialized with RC ATMOS data. Layout is as in Plate 10b. The black triangle indicates the location of the HALOE profile in Plate 11a.

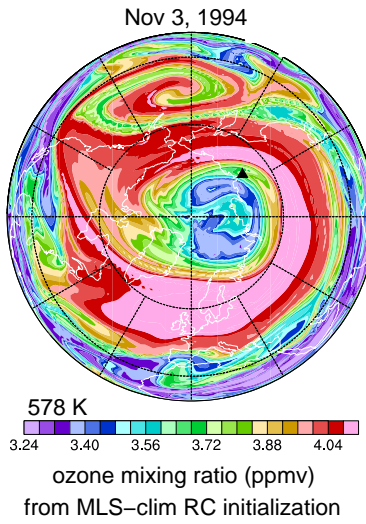


Plate 12. RT map of ozone at 578 K initialized with RC MLS climatology data at the time of the POAM II observation inside the vortex shown in Plate 9 (black triangle). Layout is as in Plate 10b.

inae in the observations. Plate 13 shows RT maps at 743 K for each of these profiles; the laminae in the RT profiles arose from sampling in a region of inhomogeneous ozone well within the vortex. The details of the shape and size of this region vary between the instruments. Manney et al. [1998] showed that RT calculations initialized with reconstructed PV/ θ space fields were often unsuccessful in reproducing laminae arising from advection of such localized features within the polar vortex, as the averaging of features not well correlated with PV can lead to patterns in the RC fields that may not strongly resemble localized features present in the atmosphere. These results suggest that the observed laminae, which appear in several independent measurements, may arise from advection within the vortex of local ozone features that are only incompletely captured in the RC initialization fields.

The above examples detail the atmospheric origins of laminae seen in profiles observed by multiple instruments in close proximity, demonstrating that many of these laminae arise from differential advection of ozone by the large-scale winds. Appearance of such laminae in coincident observations by multiple instruments demonstrates detailed agreement between those instruments.

6. Summary and Conclusions

Equivalent latitude/potential temperature (EqL/ θ) ozone fields in early November 1994 constructed from seven satellite instruments' (the ATMOS, SAGE II, POAM II, and HALOE solar occultation instruments and the MLS, CRISTA, and MAS limb-emission instruments) data show very good agreement in both the upper and the lower stratosphere. Values usually agree to within 0.5 ppmv ($\sim 5\%$) in the upper stratosphere, where chemical processes are the dominant factor driving short timescale changes in ozone. In the lower stratosphere all instruments' ozone values usually agree to within 0.25 ppmv; isolated regions with larger differences occur along the vortex edge, where very strong ozone and PV gradients magnify uncertainties in the EqL/ θ mapping. All instruments that observed in the SH polar vortex (ATMOS, SAGE II, POAM II, MLS, and CRISTA) showed a slight depression in the ozone contours along the vortex edge in the lower stratosphere, resulting from greater diabatic descent and less chemical ozone loss there. Good agreement between all these instruments in the Antarctic ozone hole indicates that, by late spring, the ozone loss that occurred earlier has been mixed sufficiently throughout the vortex to be well correlated with PV. ATMOS, SAGE II, POAM II, and MLS all show ozone values less than 0.25 ppmv below 420 K in the ozone hole region (CRISTA did not retrieve ozone at this level).

Differences in the EqL/ θ fields between instruments in the middle stratosphere are usually readily explained by sampling differences. In the SH middle stratosphere, instruments with observations confined to high latitudes (ATMOS, SAGE II, and POAM II) measured low EqL (low PV) in air that had been drawn up from low latitudes and confined in an anticyclone. A low-ozone pocket [Manney et al., 1995] had formed in this region as the confined ozone relaxed chemically toward equilibrium values for higher latitudes [Nair et al., 1998; Morris et al., 1998]. Thus those instruments measured much lower ozone at low EqL than the limb-emission instruments, whose low EqL ozone was a mixture of observations at low latitudes and in the low-ozone pocket region. HALOE, which observed only the tropics in the SH, showed even higher ozone values at low EqL.

A low-ozone pocket had also formed in the NH middle stratosphere. Although a low-ozone pocket has not been reported previously before mid-December in the NH, its appearance is consistent with the NH circulation in early November 1994, wherein a minor warming event led to low-latitude air being drawn up around the protovortex and into the developing anticyclone [Manney et al., 2000]. ATMOS, HALOE, and SAGE II, observing at latitudes up to the protovortex edge region, sampled a mixture of air from fila-

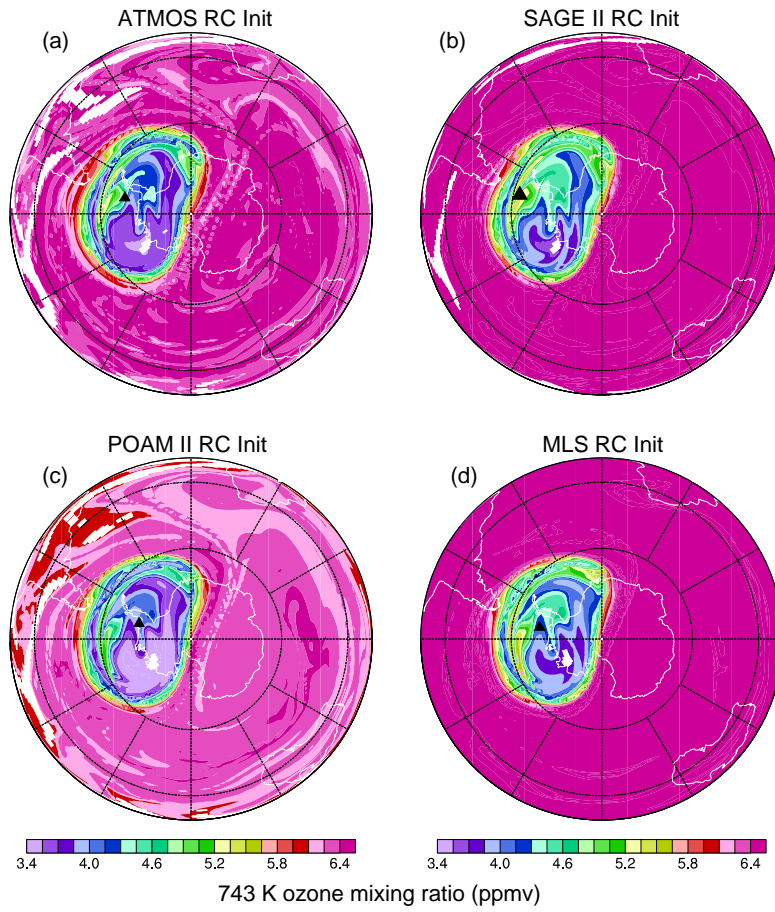


Plate 13. RT ozone maps at 743 K at the times of the four profiles shown in the top left panel of Plate 6, initialized with RC data from (a) ATMOS, (b) SAGE II, (c) POAM II, and (d) MLS. The map projection is orthographic, with 0°longitude at the top and 90°E to the right. The domain is from equator to pole, with thin dashed lines at 30° and 60°S. Black triangles show locations of corresponding observations.

ments drawn off the protovortex, the low ozone pocket, and low-latitude air that was being drawn up around the vortex. Ozone from these instruments in mid-EqL is higher than that from POAM II, which sampled only at very high ($\sim 68^\circ\text{N}$) latitudes, where extravortex air sampled did not include any tropical, high-ozone tongues. SAGE II mid-EqL ozone was lower because it did not sample the tropics, but sampled low-EqL air only in the low-ozone pocket.

Comparisons of the observations in the low-ozone pocket give a clear example of a situation where chemical processes result in a poor correlation between PV and ozone. The substantial differences between instruments in the mid-EqL middle stratosphere resulting from sampling differences are a reminder of the care that must be taken to understand the relationship between PV and gases with short lifetimes in applying comparison methods based on air mass coincidence.

When care is taken to match PV between instruments, individual profile comparisons show overall remarkably good agreement between all instruments with sampling at similar latitudes. Some small discrepancies still result from sampling differences, where profiles with closely matching longitudes could not be found in the midlatitude middle stratosphere. Differences that cannot be attributed to sampling include some MLS extravortex profiles in the SH with $\sim 10\%$ higher values at the mixing ratio peak than other instruments to which they were compared (EqL/θ fields from MLS also show values $\sim 5\text{--}15\%$ higher than CRISTA and MAS in SH mid-EqLs at the mixing ratio peak). Also, the NH tropical profile from CRISTA was $\sim 10\text{--}15\%$ lower at the peak than those from ATMOS, SAGE II, MLS, and MAS (consistent with the difference seen between CRISTA and other instruments with good tropical coverage in the EqL/θ fields); this difference suggests the possibility of a slight low bias in CRISTA in the tropical midstratosphere. Even these differences, however, are generally less than estimates of the total uncertainties for the instruments.

The individual profiles compared showed small vertical scale laminae, with similar features appearing in profiles from several instruments that had close coincidences in PV, latitude, and longitude. Reverse trajectory (RT) calculations show that many of these laminae in the NH arise from filamentation in and around the Arctic protovortex, confirming the conclusions of Manney et al. [2000]. RT calculations suggest that laminae seen in several instruments' profiles inside the SH vortex may arise from local variations in ozone that, since they are not well-correlated with PV, are not accurately represented in the EqL/θ fields used for initialization. The RT calculations provide confirmation of the atmospheric origin of these laminae; that such laminae appear in several instruments' profiles demonstrates detailed agreement between these instruments.

It is difficult to compare observations of ozone, which has a short chemical lifetime in much of the stratosphere, between instruments with very different sampling patterns. The EqL/θ comparisons indicate that comparing values observed in equivalent air masses (i.e., as a function of EqL) can, however, be successful in the upper stratosphere (where chemistry dominates), and in the lower stratosphere (where dynamics dominates). Although these comparisons are more complicated in the middle stratosphere, careful examination of these fields, with attention to the effects of different sampling, can provide useful information on the ozone observations from various instruments. Furthermore, profile comparisons, with care taken to compare only similar air masses, proved very useful in indicating overall agreement between ozone from all of the instruments. That all seven of these instruments show remarkably good overall agreement in ozone values under a variety of meteorological conditions covering most of the globe and the full depth of the stratosphere gives high confidence in the value of all of these data sets for detailed studies of ozone photochemistry, transport, and climatology.

Acknowledgments. We thank the ATMOS, SAGE II, POAM II, HALOE, MLS, CRISTA, and MAS instrument teams for their role in producing those data sets, and the Met Office for meteorological data. Thanks to Lucien Froidevaux, Cora Randall, and Michelle Santee for valuable comments and discussions. Work at the Jet Propulsion Laboratory, California Institute of Technology, was done under contract with the National Aeronautics and Space Administration. H.A.M. was supported by the NASA Atmospheric Chemistry, Modeling, and Analysis Program (NAS1-98118).

References

- Bacmeister, J. T., V. Kuell, D. Offermann, M. Riese, and J. W. Elkins, Intercomparison of satellite and aircraft observations of ozone, CFC-11, and NO_y using trajectory mapping, *J. Geophys. Res.*, 104, 16,379–16,390, 1999.
- Barath, F. T., et al., The Upper Atmosphere Research Satellite Microwave Limb Sounder Instrument, *J. Geophys. Res.*, 98, 10,751–10,762, 1993.
- Brasseur, G., and S. Solomon, *Aeronomy of the Middle Atmosphere*, 2nd ed., D. Reidel, Norwell, Mass., 1986.
- Brühl, C., et al., Halogen Occultation Experiment ozone channel validation, *J. Geophys. Res.*, 101, 10,217–10,240, 1996.
- Butchart, N., and E. E. Remsberg, The area of the stratospheric polar vortex as a diagnostic for tracer transport on an isentropic surface, *J. Atmos. Sci.*, 43, 1319–1339, 1986.
- Chu, W. P., M. P. McCormick, J. Lenoble, C. Brogniez,

- and P. Pruvost, SAGE II inversion algorithm, *J. Geophys. Res.*, 94, 8339–8351, 1989.
- Cunnold, D. M., W. P. Chu, R. A. Barnes, M. P. McCormick, and R. E. Veiga, Validation of SAGE II ozone measurements, *J. Geophys. Res.*, 94, 8447–8460, 1989.
- Cunnold, D. M., H. Wang, W. P. Chu, and L. Froidevaux, Comparisons between Stratospheric Aerosol and Gas Experiment II and Microwave Limb Sounder ozone measurements and aliasing of SAGE II ozone trends in the lower stratosphere, *J. Geophys. Res.*, 101, 10,061–10,075, 1996.
- Daehler, M., et al., Validation of Millimeter-wave Atmospheric Sounder (MAS) ozone measurements, *J. Geophys. Res.*, 103, 19,615–19,639, 1998.
- Deniel, C., et al., A comparative study of POAM II and electrochemical concentration cell ozonesonde measurements obtained over northern Europe, *J. Geophys. Res.*, 102, 23,629–23,642, 1997.
- Dunkerton, T. J., and D. P. Delisi, Evolution of potential vorticity in the winter stratosphere of January–February 1979, *J. Geophys. Res.*, 91, 1199–1208, 1986.
- Froidevaux, L., et al., Validation of the UARS Microwave Limb Sounder ozone measurements, *J. Geophys. Res.*, 101, 10,017–10,060, 1996.
- Glaccum, W., et al., The Polar Ozone and Aerosol Measurement instrument, *J. Geophys. Res.*, 101, 14,479–14,487, 1996.
- Gunson, M. R., et al., The Atmospheric Trace Molecule Spectroscopy (ATMOS) experiment: Deployment on the ATLAS Space Shuttle missions, *Geophys. Res. Lett.*, 23, 2333–2336, 1996.
- Hartmann, G. K., et al., Measurements of O₃, H₂O, and ClO in the middle atmosphere using the Millimeter-wave Atmospheric Sounder (MAS), *Geophys. Res. Lett.*, 23, 2313–2316, 1996.
- Juckes, M. N., and A. O'Neill, Early winter in the Northern Hemisphere, *Q. J. R. Meteorol. Soc.*, 114, 1111–1125, 1988.
- Knox, J. A., On converting potential temperature to altitude in the middle atmosphere, *Eos Trans. AGU*, 79, 376, 1998.
- Lary, D. J., M. P. Chipperfield, J. A. Pyle, W. A. Norton, and L. P. Riishojaard, Three-dimensional tracer initialization and general diagnostics using equivalent PV latitude-potential-temperature coordinates, *Q. J. R. Meteorol. Soc.*, 121, 187–210, 1995.
- Lingenfelser, G. S., W. L. Grose, E. E. Remsberg, T. D. Fairlie, and R. B. Pierce, Comparison of satellite and in situ ozone measurements in the lower stratosphere, *J. Geophys. Res.*, 104, 13,971–13,979, 1999.
- Lu, C.-H., G. K. Yue, G. L. Manney, H. Jaeger, and V. A. Mohnen, Lagrangian approach for Stratospheric Aerosol and Gas Experiment (SAGE) II profile intercomparisons, *J. Geophys. Res.*, 105, 4563–4572, 2000.
- Lumpe, J. D., et al., POAM II retrieval algorithm and error analysis, *J. Geophys. Res.*, 102, 23,593–23,614, 1997.
- Manney, G. L., R. W. Zurek, A. O'Neill, and R. Swinbank, On the motion of air through the stratospheric polar vortex, *J. Atmos. Sci.*, 51, 2973–2994, 1994a.
- Manney, G. L., R. Swinbank, and A. O'Neill, Stratospheric meteorological conditions for the 3–12 Nov 1994 ATMOS/ATLAS-3 measurements, *Geophys. Res. Lett.*, 23, 2409–2412, 1996.
- Manney, G. L., J. C. Bird, D. P. Donovan, T. J. Duck, J. A. Whiteway, S. R. Pal, and A. I. Carswell, Modeling ozone laminae in ground-based Arctic wintertime observations using trajectory calculations and satellite data, *J. Geophys. Res.*, 103, 5797–5814, 1998.
- Manney, G. L., H. A. Michelsen, M. L. Santee, M. R. Gunson, F. W. Irion, A. E. Roche, and N. J. Livesey, Polar vortex dynamics during spring and fall diagnosed using trace gas observations from the Atmospheric Trace Molecule Spectroscopy instrument, *J. Geophys. Res.*, 104, 18,841–18,866, 1999.
- Manney, G. L., H. A. Michelsen, F. W. Irion, M. R. Gunson, G. C. Toon, and A. E. Roche, Lamination and polar vortex development in fall from ATMOS long-lived trace gases observed during November 1994, *J. Geophys. Res.*, 105, 29,023–29,038, 2000.
- Manney, G. L., et al., Chemical depletion of ozone in the Arctic lower stratosphere during winter 1992–93, *Nature*, 370, 429–434, 1994b.
- Manney, G. L., et al., Formation of low-ozone pockets in the middle stratospheric anticyclone during winter, *J. Geophys. Res.*, 100, 13,939–13,950, 1995.
- McCormick, M. P., J. M. Zawodny, R. E. Veiga, J. C. Larsen, and P. H. Wang, An overview of SAGE I and SAGE II ozone measurements, *Planet. Space Sci.*, 37, 1567–1586, 1989.
- Morris, G. A., S. R. Kawa, A. R. Douglass, M. R. Schoeberl, L. Froidevaux, and J. W. Waters, Low-ozone pockets explained, *J. Geophys. Res.*, 103, 3599–3610, 1998.
- Morris, G. A., J. F. Gleason, J. Ziemke, and M. R. Schoeberl, Trajectory mapping: A tool for validation of trace gas observations, *J. Geophys. Res.*, 105, 17,875–17,894, 2000.
- Nair, H., M. Allen, L. Froidevaux, and R. W. Zurek, Localized rapid ozone loss in the northern winter stratosphere: An analysis of UARS observations, *J. Geophys. Res.*, 103, 1555–1571, 1998.

- Offermann, D., K. U. Grossmann, P. Barthol, P. Knieling, M. Riese, and R. Trant, Cryogenic Infrared Spectrometers and Telescopes for the Atmosphere (CRISTA) experiment and middle atmosphere variability, *J. Geophys. Res.*, 104, 16,311–16,325, 1999.
- Redaelli, G., et al., UARS MLS O₃ soundings compared with lidar measurements using the conservative coordinates reconstruction technique, *Geophys. Res. Lett.*, 21, 1535–1538, 1994.
- Riese, M., R. Spang, P. Preusse, M. Ern, M. Jarisch, D. Offermann, and K. U. Grossmann, Cryogenic Infrared Spectrometers and Telescopes for the Atmosphere (CRISTA) data processing and atmospheric temperature and trace gas retrieval, *J. Geophys. Res.*, 104, 16,349–16,367, 1999.
- Rosier, S. M., B. N. Lawrence, D. G. Andrews, and F. W. Taylor, Dynamical evolution of the northern stratosphere in early winter 1991/92, as observed by the Improved Stratospheric and Mesospheric Sounder, *J. Atmos. Sci.*, 51, 2783–2799, 1994.
- Rusch, D. W., et al., Validation of POAM ozone measurements with coincident MLS, HALOE, and SAGE II observations, *J. Geophys. Res.*, 102, 23,615–23,627, 1997.
- Russell, J. M., III, et al., The Halogen Occultation Experiment, *J. Geophys. Res.*, 98, 10,777–10,797, 1993.
- Schoeberl, M. R., L. R. Lait, P. A. Newman, and J. E. Rosenfield, The structure of the polar vortex, *J. Geophys. Res.*, 97, 7859–7882, 1992.
- Schoeberl, M. R., M. Luo, and J. E. Rosenfield, An analysis of the Antarctic Halogen Occultation Experiment trace gas observations, *J. Geophys. Res.*, 100, 5159–5172, 1995.
- Schoeberl, M. R., et al., Reconstruction of the constituent distribution and trends in the Antarctic polar vortex from ER-2 flight observations, *J. Geophys. Res.*, 94, 16,815–16,845, 1989.
- Stratospheric Processes and Their Role in Climate (SPARC), SPARC/IO₃C/GAW assessment of trends in the vertical distribution of ozone, World Meteorol. Org. Global Ozone Res. and Monit. Proj., Geneva, Switzerland, 1998.
- Sutton, R. T., H. MacLean, R. Swinbank, A. O'Neill, and F. W. Taylor, High-resolution stratospheric tracer fields estimated from satellite observations using Lagrangian trajectory calculations, *J. Atmos. Sci.*, 51, 2995–3005, 1994.
- Wang, H. J., D. M. Cunnold, L. Froidevaux, and J. M. Russell III, A reference model for middle atmosphere ozone in 1992/1993, *J. Geophys. Res.*, 104, 21,629–21,643, 1999.
- World Meteorological Organization, Scientific assessment of stratospheric ozone, 1998, U. N. Environ. Program, Geneva, Switzerland, 1999.
-
- R. M. Bevilacqua, Naval Research Laboratory, Code 7220, Washington, DC 20375.
- M. R. Gunson, Jet Propulsion Laboratory, Mail Stop 169-237, Pasadena, CA 91109.
- F. W. Irion and G. C. Toon, Jet Propulsion Laboratory, Mail Stop 183-601, Pasadena, CA 91109.
- N. J. Livesey, Jet Propulsion Laboratory, Mail Stop 183-701, Pasadena, CA 91109.
- G. L. Manney, Department of Physics, New Mexico Highlands University, Las Vegas, NM 87701. (manney@mls.jpl.nasa.gov).
- H. A. Michelsen, Combustion Research Facility, Sandia National Laboratories, MS 9055, P.O. Box 969, Livermore, CA 94551.
- J. Oberheide and M. Riese, Physics Department (D 07.05), University of Wuppertal, Gaussstr. 20, D-42097 Wuppertal, Germany.
- J. M. Russell III, Center for Atmospheric Sciences, Hampton University, P.O. Box 6075, Hampton, VA 23668.
- J. M. Zawodny, NASA Langley Research Center, Mail Stop 475, 23a Langley Boulevard, Hampton, VA 23681.

September 14, 2000; revised December 13, 2000; accepted December 14, 2000.

This preprint was prepared with AGU's L^AT_EX macros v4, with the extension package 'AGU⁺⁺' by P. W. Daly, version 1.5g from 1998/09/14.